Risau W. 1995. Differentiation of endothelium. FASEB J 9:926–933.
Risau W, Flamme I. 1995. Vasculogenesis. Annu Rev Cell Dev Biol 11:73–91.
Shalaby F, Ho J, Stanford WL, Fischer KD, Schuh AC, Schwartz L, Bernstein A, Rossant J. 1997. A requirement for Flk1 in primitive and definitive hematopoiesis and vasculogenesis. Cell 89:981–990.
Shimizu R, Takahashi S, Ohneda K, Engel JD, Yamamoto M. 2001. In vivo requirements for GATA-1 functional domains during primitive and definitive erythropoiesis. EMBO J 20:5250–5260.
Shimizu R, Kuroha T, Ohneda O, Pan X, Ohneda K, Takahashi S, Philipsen S, Yamamoto M. 2004. Leukemogenesis caused by incapacitated GATA-1 function. Mol Cell Biol 24:10814–10825.
Shinoda G, Umeda K, Heike T, Arai M, Niwa A, Ma F, Suemori H, Luo HY, Chui DH, Torii R, Shibuya M, Nakatsuji N, Nakahata T. 2007. alpha4-Integrin(+) endothelium derived from primate embryonic stem cells generates primitive and definitive hematopoietic cells. Blood 109:2406–2415.
Suwabe N, Takahashi S, Nakano T, Yamamoto M. 1998. GATA-1 regulates growth and differentiation of definitive erythroid lineage cells during in vitro ES cell differentiation. Blood 92:4108–4118.
Takahashi K, Yamanaka S. 2006. Induction of pluripotent stem cells from mouse embryonic and adult fibroblast cultures by defined factors. Cell 126:663–676.
Takahashi K, Tanabe K, Ohnuki M, Narita M, Ichisaka T, Tomoda K, Yamanaka S. 2007. Induction of pluripotent stem cells from adult human fibroblasts by defined factors. Cell 131:861–872.
Umeda K, Heike T, Yoshimoto M, Shiota M, Suemori H, Luo HY, Chui DH, Torii R, Shibuya M, Nakatsuji N, Nakahata T. 2004. Development of primitive and definitive hematopoiesis from nonhuman primate embryonic stem cells in vitro. Development (Cambridge, England) 131:1869–1879.
Umeda K, Heike T, Yoshimoto M, Shinoda G, Shiota M, Suemori H, Luo HY, Chui DH, Torii R, Shibuya M, Nakatsuji N, Nakahata T. 2006. Identification and characterization of hemoangiogenic progenitors during cynomolgus monkey embryonic stem cell differentiation. Stem Cells (Dayton, Ohio) 24:1348–1358.
van de Rijn M, Heimfeld S, Spangrude GJ, Weissman IL. 1989. Mouse hematopoietic stem-cell antigen Sca-1 is a member of the Ly-6 antigen family. Proc Natl Acad Sci USA 86:4634–4638.
Vodyanik MA, Slukvin II. 2007. Hematoendothelial differentiation of human embryonic stem cells. Curr Protoc Cell Biol Chapter 23:Unit 23.6.
Vodyanik MA, Bork JA, Thomson JA, Slukvin II. 2005. Human embryonic stem cell-derived CD34+ cells: Efficient production in the coculture with OP9 stromal cells and analysis of lymphohematopoietic potential. Blood 105:617–626.
Wood HB, May G, Healy L, Enver T, Morriss-Kay GM. 1997. CD34 expression patterns during early mouse development are related to modes of blood vessel formation and reveal additional sites of hematopoiesis. Blood 90:2300–2311.
Woodard JP, Gulbahce E, Shreve M, Steiner M, Peters C, Hite S, Ramsay NK, DeFor T, Baker KS. 2000. Pulmonary cytolytic thrombi: A newly recognized complication of stem cell transplantation. Bone Marrow Transplant 25:293–300.
Xu MJ, Matsuoka S, Yang FC, Ebihara Y, Manabe A, Tanaka R, Eguchi M, Asano S, Nakahata T, Tsuji K. 2001. Evidence for the presence of murine primitive megakaryocytopoiesis in the early yolk sac. Blood 97:2016–2022.
Yamashita J, Itoh H, Hirashima M, Ogawa M, Nishikawa S, Yurugi T, Naito M, Nakao K. 2000. Flk1-positive cells derived from embryonic stem cells serve as vascular progenitors. Nature 408:92–96.
Yang FC, Tsuji K, Oda A, Ebihara Y, Xu MJ, Kaneko A, Hanada S, Mitsui T, Kikuchi A, Manabe A, Watanabe S, Ikeda Y, Nakahata T. 1999. Differential effects of human granulocyte colony-stimulating factor (hG-CSF) and thrombopoietin on megakaryopoiesis and platelet function in hG-CSF receptor-transgenic mice. Blood 94:950–958.
Yu J, Vodyanik MA, Smuga-Otto K, Antosiewicz-Bourget J, Frane JL, Tian S, Nie J, Jonsdottir GA, Ruotti V, Stewart R, Slukvin II, Thomson JA. 2007. Induced pluripotent stem cell lines derived from human somatic cells. Science (New York, NY) 318:1917–1920.

Biochemical and Biophysical Research Communications 377 (2008) 205–209

Contents lists available at ScienceDirect

Biochemical and Biophysical Research Communications

journal homepage: www.elsevier.com/locate/ybbrc

Expression profile analysis of aorta-gonad-mesonephros region-derived stromal cells reveals genes that regulate hematopoiesis

Kenji Nagao [a], Takayuki Ohta [b], Atsushi Hinohara [b], Tomoyuki Tahara [b], Tetsuya Hagiwara [a], Yoshitake Maeda [a], Takashi Yoneya [b], Yoshiaki Sohma [b], Toshio Heike [c], Tatsutoshi Nakahata [c], Yoshimasa Inagaki [b,*], Mitsuo Nishikawa [b,1]

[a] Frontier Laboratory, Kirin Pharma CO., LTD., 3 Miyahara, Takasaki, Gunma 370-1295, Japan
[b] Discovery Research Laboratories, Kirin Pharma CO., LTD., 3 Miyahara, Takasaki, Gunma 370-1295, Japan
[c] Department of Pediatrics, Graduate School of Medicine, Kyoto University, 54 Kawahara-cho, Shogoin, Sakyo-ku, Kyoto 606-8507, Japan

ARTICLE INFO

Article history:
Received 18 September 2008
Available online 7 October 2008

Keywords:
AGM
Stroma
Glypican
Hematopoietic stem cell

ABSTRACT

The aorta-gonad-mesonephros (AGM) region is involved in the generation and maintenance of the first definitive hematopoietic stem cells (HSCs). A mouse AGM-derived cell line, AGM-S3, was shown to support the development of HSCs. To elucidate the molecular mechanisms regulating early hematopoiesis, we obtained subclones from AGM-S3, one of which was hematopoiesis supportive (S3-A9) and the other one of which was non-supportive (S3-A7), and we analyzed their gene expression profiles by gene chip analysis. In the present study, we found that Glypican-1 (GPC1) was highly expressed in the supportive subclone AGM-S3-A9. Over-expression of GPC1 in non-supportive cells led to the proliferation of progenitor cells in human cord blood when cocultured with the transfected-stromal cells. Thus, GPC1 may have an important role in the establishment of a microenvironment that supports early events in hematopoiesis.

© 2008 Elsevier Inc. All rights reserved.

Hematopoiesis is regulated by the close interaction between hematopoietic cells and the hematopoiesis supporting microenvironment in a hematopoietic organ, such as bone marrow. Stromal cells are major components of the microenvironment and they provide hematopoietic cells with factors that regulate differentiation and proliferation [1–3]. For example, recent studies have demonstrated that osteoblastic cells play important roles for HSC maintenance and Ang-1, a Tie2 ligand, plays crucial role in hematopoietic stem cell maintenance [4].

Heparan sulphate proteoglycans (HSPGs) are reported to be involved in the establishment of the microenvironmental niche and mediate the interaction between HSCs and stromal cells [5]. It is postulated that cell-surface molecules such as CD45, PECAM-1, and Thy-1, which are known heparin-binding proteins, cooperatively contribute to form the hematopoietic niche by presenting growth factors, and they further serve as co-receptors for the growth factors [6–8].

During the embryonic development of the mouse, the first definitive hematopoietic stem cells (HSCs) emerge in the aorta-gonad-mesonephros (AGM) region at E10.5 and thereafter shift to the fetal liver (FL) at E12.5 [9–11]. We previously reported the establishment of stromal cell lines from the AGM region of an E10.5 mouse embryo and one of the cell lines, AGM-S3, was shown to be capable of supporting hematopoiesis [12]. Moreover, E8 yolk sac cells, which normally have no repopulating ability, were shown to mature into long-term repopulating HSCs upon coculture with AGM-S3. This observation suggests that the microenvironment of the stromal cells, derived from the E10.5 AGM region, is important for the generation of long term repopulating-HSCs and that AGM-S3 cells can be used to elucidate the molecular mechanisms regulating early hematopoiesis.

Here, we established cell lines with varying hematopoietic supporting abilities from AGM-S3. Gene chip analysis of the established supportive and non-supportive cell lines revealed a large proportion of genes up-regulated in the supportive cell line which could be involved in cell–cell interactions. Through the forced expression of these candidate genes in the non-supportive subclone, we show that GPC1, a member of HSPG family, can confer hematopoiesis supporting activity to non-supportive stromal cells.

Materials and methods

Cell preparation. AGM-S3 was subcultured in MEMα medium (Invitrogen Corp., Carlsbad, CA) supplemented with inactive 10% fetal calf serum (FCS, HyClone Laboratories, Inc., UT). Subcloning

* Corresponding author. Fax: +81 27 346 1971.
E-mail address: yoshimasa.inagaki@kyowa-kirin.co.jp (Y. Inagaki).
[1] Present address: Interprotein Corporation, SIC-1-202, 5-4-21 Nishihashimoto, Sagamihara, Kanagawa, 229-1131, Japan.

0006-291X/$ - see front matter © 2008 Elsevier Inc. All rights reserved.
doi:10.1016/j.bbrc.2008.09.123

was performed by sorting cells using a cell sorter (FACS Vantage; Becton Dickinson Biosciences, San Jose, CA) and plating them in a 96-well plate (BD Falcon, Bedford, MA) at an expected density of one cell per well. Human umbilical cord blood cells were obtained and manipulated with informed written consent in accordance with the Declaration of Helsinki and with permission from the institutional ethics committee of Kirin Pharma Co., Ltd. Mononuclear cells were separated by Ficoll density gradient centrifugation using Lymphoprep (Nycomed Pharma). Differentiated blood cells, which expressed differentiation antigens, CD2, CD11c, CD19, CD15, and CD41, and Glycophorin A, were removed using the Dynal MPC-1 magnetic separator (Dynal Biotech, Norway). $CD34^+$ or $CD34^+$ $CD38^-$ cells were recovered using a cell sorter after labeling with FITC-conjugated anti-CD34 and PC5-conjugated anti-CD38 antibodies (Immunotech). Bone marrow cells were collected from the femur of male C57BL/6-Ly5.1 pep mice (ages ranging from eight to ten weeks) and suspended in PBS and the hematopoietic stem cell fraction was obtained as described previously [13,14]. $CD34^-$, $Sca\text{-}1^+$, $c\text{-}Kit^+$, Lin^- cell population was separated using a cell sorter. GPC1 expression was detected using a rat-anti-mouse GPC1 monoclonal antibody and visualized using a PE- labeled anti-Rat IgG (BD Bioscience, CA). All studies using animals were reviewed and approved by the Institutional Animal Care and Use Committee at the Discovery Research Laboratories of Kirin Pharma Co. Ltd.

Colony-forming assay. Coculture of human hematopoietic stem cells with stromal cells and methylcellulose clonal culture was performed using a modification of the technique described previously [12].

The analysis was performed with the addition of 10 ng/ml of human SCF, human IL-3, human IL-6, human G-CSF, human TPO, and EPO at 2 IU/ml to MethoCult H4230 (Stem Cell Technologies Inc., Vancouver, BC, Canada). The abbreviations used for the colony-forming assay are as follows: BFU-E, erythroid burst-forming units; CFU-GM, granulocyte-macrophage colony-forming units; CFU-E mix, mixed colony-forming units.

Transplantation assay. AGM-derived stromal cell lines (AGM-S3-A9 and AGM-S3-A7); OP9 cells (RCB1124, RIKEN Cell Development Bank); L929 cell (ATCC); or NIH3T3 cells (ATCC) were seeded in a 48-well culture dish (BD Falcon, MA) at 5×10^4 cells/well and cultured in MEMα medium (Invitrogen, CA) containing 10% FCS (HyClone, UT) for three days. A total of 30 pre-sorted mouse hematopoietic stem cells (derived from C57BL/6-Ly5.1) per well were added to the stromal cells ($n = 5$). After 7 days of coculture, the cells were trypsinized and recovered. The whole recovered cells (30 34^-KSL cells equivalent) were then mixed with 3000 Lin-negative bone marrow cells derived from C57BL/6-Ly5.2 mouse (Charles River) and introduced via the tail vein into a C57BL/6-Ly5.2 mouse (eight weeks age and male, Charles River) that had been irradiated with X-rays at 8.5 Gy. The peripheral blood cells were isolated and those derived from the C57BL/6-Ly5.1 mice were detected by FACS using previously described methods [14].

Gene chip expression analysis. Genome-wide gene expression was examined using the Mouse Genome MG-U74A, B, C Probe array (GeneChip, Affymetrix, Inc., USA). Assays were performed according to the manufacturer's protocol. Total RNA was isolated from each stromal cell lines with an RNeasy mini-kit (Qiagen, Chatsworth, CA). GeneChip software was used to determine the average difference (AD) in the levels of gene expression among genes on the array. The mean ADs for 3′-terminal probe sets corresponding to four constitutively expressed genes (β-actin, GAPDH, pyruvate carboxylase and transferrin receptor) were calculated, and hereafter, we use STD to refer to the mean AD of the control probe set. To normalize staining intensity among chips, the AD values for all genes on a given chip were divided by the ratio of the STD for each chip to the average STD for all chips. Normalized AD values less than 0.1 were set to 0.1. Then, the dataset was sorted by the ratio of the mean AD of each gene in a target group to that in a reference group in order to identify highly expressed genes within an experimental group.

Transfection into plat-E cells and retroviral infection of stromal cells. The PCR amplified GPC1 cDNAs were subcloned into the plasmid vector pMX/IRES/GFP (pMXIG) or pLRT. The pMXIG or pLRT-derived plasmid vectors were transfected into PLAT-E cells using FuGene6 (Roche Diagnostics GmbH, Mannheim, Germany) [15]. After a 48-h culture, the supernatants were collected and centrifuged at 6000*g* for 16 h at 4 °C to enrich virus particles. The stromal cell culture medium was replaced with virus-containing media. GFP positive pMXIG transfectants were sorted and used in the coculture assay. The GPC1-A7 cell populations were obtained by positive cell sorting in the presence of doxycycline (Dox) (500 μg/ml) and negative cell sorting in the absence of Dox.

Reverse transcriptase PCR. Total RNA was extracted from AGM-S3-A9, AGM-S3-A7, OP9 or NIH3T3 and subjected to PCR. Oligonucleotide primer sequences used were as follows: GPC1 forward, 5′-CC TGGCTTACCAAGGCTGTCA-3′, and GPC1 reverse, 5′-GTGCTGGCAATA GCCTCTCTAAC-3′; GAPDH forward, 5′-ACCACAGTCCATGCCATCAC-3′, and GAPDH reverse, 5′-TCCACCACCCTGTTGCTGTA -3′.

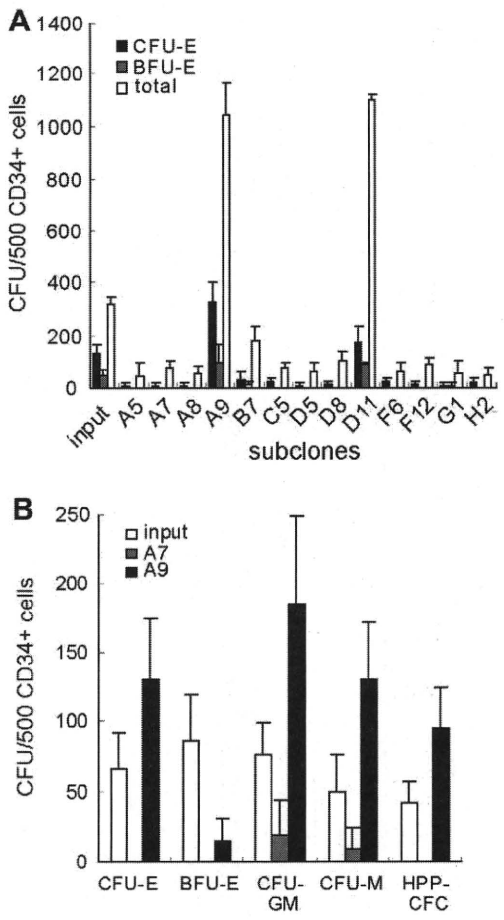

Fig. 1. Subcloning of AGM-S3 stromal cells. (A) Coculture of human CB $CD34^+$ cells with AGM-S3 derived subclones. Human CB $CD34^+$ cells (500 per well) were added to the stromal cells and cultured for two weeks. Clonogenic progenitors were evaluated by culturing a fraction of the cells after they were harvested. Colonies were counted at day 14. (B) Coculture of human CB $CD34^+$ cells with AGM-S3-A9 and AGM-S3-A7.

Results and discussion

Establishment of the subclones from AGM-S3 stromal cells

We previously reported the establishment and characteristics of the stromal cell line AGM-S3, which was generated from the AGM region of an E10.5 mouse embryo [12]. However, since the cell line might be unstable through repeated passages, we tried to obtain stable subclones. We isolated thirteen proliferative subclones from ninety six single-sorted AGM-S3 cells. According to the method for establishment of AGM-S3, we evaluated their hematopoiesis supporting ability by coculture with human hematopoietic progenitor cells (HPCs) (CB $CD34^+$ cells). The results of the clonal assays showed that eleven clones had no effect on hematopoiesis and the remaining two clones supported hematopoiesis (Fig. 1A). One of the non-supportive eleven, AGM-S3-A7, and one of the supportive two, AGM S3-A9, were more stable than the others.

After 14 days of coculture, the number of colony-forming cells (CFU-Cs) increased 3.4-fold in the coculture with AGM-S3-A9, whereas the effect of AGM-S3-A7 was very poor. In subsequent clonogenic experiments, AGM-S3-A9 supported proliferation of several different types of progenitor cells, including CFU-GM, BFU-E, and CFU-E mix (Fig. 1B). Taken together, these results indicate that AGM-S3-A9 has the potential to support human hematopoiesis, but AGM-S3-A7 does not.

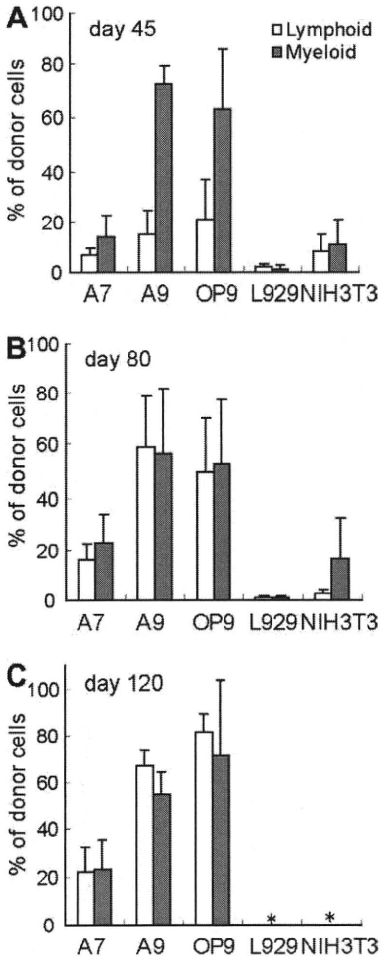

Fig. 2. Hematopoietic reconstitution via coculture of mouse BM 34-KSL cells with AGM-S3-A7, AGM-S3-A9, OP9, L929, or NIH3T3 cells. The cocultured 34-KSL cells were transplanted into a group of lethally irradiated mice ($n=5$). The percentage of Ly-5.1$^+$ cells in lymphoid cells (Thy-1$^+$ and B220$^+$) and in myeloid cells (Gr-1$^+$ and CD11c$^+$) were determined from the peripheral blood of Ly-5.2 recipient mice at (A) 45, (B) 80 days, and (C) 120 Days post-transplantation. *, no mouse survived.

To investigate the effect of the newly established cell lines on murine HSCs that have long-term repopulating ability (LTR-HSCs), we cocultured Lin$^-$, c-Kit$^+$, Sca-1$^+$, CD34$^-$ cells (34$^-$ KSL cells) from the adult bone marrow with AGM-S3-A9 cells, AGM-S3-A7 cells, OP9, L929, or NIH3T3 cell lines. 34$^-$KSL cells cocultured with AGM-S3-A9 were able to repopulate lethally irradiated mice with high level of chimerism in the same way as OP9 cells that are known to support HSCs [16] (Fig. 2). However, HSCs cocultured with AGM-S3-A7, L929, or NIH3T3 cells could only rarely repopulate the recipient mice. Thus, the hematopoiesis supporting ability of AGM-S3-A9 cells or non-supporting ability of AGM-S3-A7 cells is relevant to human and mouse hematopoietic cells.

Comparative transcriptional profiling of AGM-S3-A9 and AGM-S3-A7 cells

We hypothesized that the genes that promote the support of hematopoiesis would be preferentially expressed in the supportive cell lines such as AGM-S3-A9 and OP9, whereas they would be less expressed in the non-supportive AGM-S3-A7. To investigate differentially regulated genes, we performed a gene chip analysis. In the present study, we focused on membrane proteins or membrane binding proteins, since conditioned medium from AGM-S3 cells showed a much reduced supportive ability as compared with coculture using whole cells [12].

As a result of the comparison between AGM-S3-A9, OP9, and AGM-S3-A7, we identified 216 up-regulated and 417 down-reg-

Table 1
Genes upregulated in AGM-s3-A9 or OP9 compared to AGM-s3-A7 cells.

Gene	GenBank	Fold change	
	Accession No.	A9/A7	OP9/A7
Cytokine-related genes			
Interleukin 1 receptor antagonist (Il1rn)	NM_031167	5.6	6.1
Stem cell factor (SCF)	NM_013598	3.5	2.9
Chemokine (C-X-C motif) ligand 12 (Cxcl12)	NM_021704	3.4	4.3
Growth arrest specific 6 (Gas6)	NM_019521	3.3	4.2
Chemokine (C-C motif) ligand 9 (Ccl9)	NM_011338	3.2	6.7
Wingless related MMTV integration site 10b (Wnt10b)	NM_011718	2.5	3.1
Fibroblast growth factor 10 (Fgf10)	NM_008002	2.3	4.6
Adipo Q (Adipoq)	NM_009605	2.3	19.1
Receptor-related genes			
G protein-coupled receptor 109A (Gpr109a)	NM_030701	11.4	30.3
Ephrin B1 (Efnb1)	NM_010110	3.4	3
PTK7 protein tyrosine kinase 7 (Ptk7)	NM_175168	2.9	2.1
Notch gene homolog 3 (Drosophila) (Notch3)	NM_008716	2.4	3
Extracellular matrix-related genes			
Procollagen, type XV (Col15a1)	NM_009928	23.5	9.4
Procollagen, type IV, alpha 1 (Col4a1)	NM_009931	5.7	2.7
Matrilin 4 (Matn4)	NM_013592	5.3	2.2
Glypican 6 (Gpc6)	NM_011821	5.3	4.5
A disintegrin and metallopeptidase domain 15 (ADAM15)	NM_009614	2.5	2.8
Glypican 1 (Gpc1)	NM_016696	2.4	2.3
Syndecan 3 (Sdc3)	NM_011520	2.1	3.7
Other			
R-spondin 3 homolog (Xenopus laevis) (Rspo3)	NM_028351	27.8	200.2
Intercellular adhesion molecule (Icam1)	NM_010493	8.8	24.7
Retinoic acid receptor responder (tazarotene induced) 2 (Rarres2)	NM_027852	5.8	3.7
Plexin domain containing 2 (Plxdc2)	NM_026162	2.3	2.5

ulated genes with at least a 2-fold increase or decrease in the average difference between the supportive and non supportive cell lines. The expression profile data were deposited in the GEO database (GSE11891). The list of genes that displayed the greatest degrees of difference and were predicted to be membrane proteins or secreted proteins is shown in Table 1. Several genes that have previously been identified as regulators of cell–cell interactions were found to be up-regulated in AGM-S3-A9, including intercellular adhesion molecule (ICAM), plexin domain containing 2 (Plxdc2), and several HSPGs. Those molecules might be involved in the interaction between HSCs and their stromal niche.

CXCL12 is also highly expressed in an AGM-derived stromal cell line established by another group [17]. CXCL12-CXCR4 signaling has been shown to be important for maintaining a pool of HSCs in the bone marrow [18] and to enhance engraftment of *in vitro* cultured HSCs to bone marrow [19]. However we observed no hematopoietic supportive activity of recombinant CXCL12 protein in AGM-S3-A7 cell coculture assays (data not shown).

Since stem cell factor (SCF), listed in Table 1, is well known as a hematopoiesis supportive factor [20,21], recombinant SCF was supplemented in the coculture of 34$^-$KSL and AGM-S3-A7 or AGM-S3-A9 and spleen colony-forming units (CFU-S) were measured. CFU-S were not altered by addition of SCF to the cocultures (Supplementary Fig. S1A). Furthermore, forced expression of SCF to AGM-S3-A7 cells did not result in an augmentation in the HSC maintenance ability of AGM-S3-A7 cells (Supplementary Fig. S1B). These findings are consistent with our previous report, in which we showed a neutralizing antibody against c-kit could reduce the number of HPCs observed in coculture with AGM-S3-A9, whereas long-term reconstitution ability was not affected by the antibody [22]. Taken together, the results suggest that SCF is required for the maintenance of HPCs and the proliferation of HSCs, but not the maintenance of HSCs.

Glypican-1 stimulates proliferation of human hematopoietic progenitor cells

Most of the up-regulated genes in the supportive cell lines could not alter the hematopoietic supporting ability of the non-supportive cells with respect to mouse CFU-S and mouse LTR-HSCs in experiments involving coculture with AGM-S3-A7 retrovirally infected with those genes. In all, seventy nine genes, including some genes listed in Table 1, were expressed and assayed for their effect on mouse or human hematopoiesis. We found that only when GPC1 was expressed in AGM-S3-A7 cells could these cells support human hematopoietic progenitor cells in a similar fashion

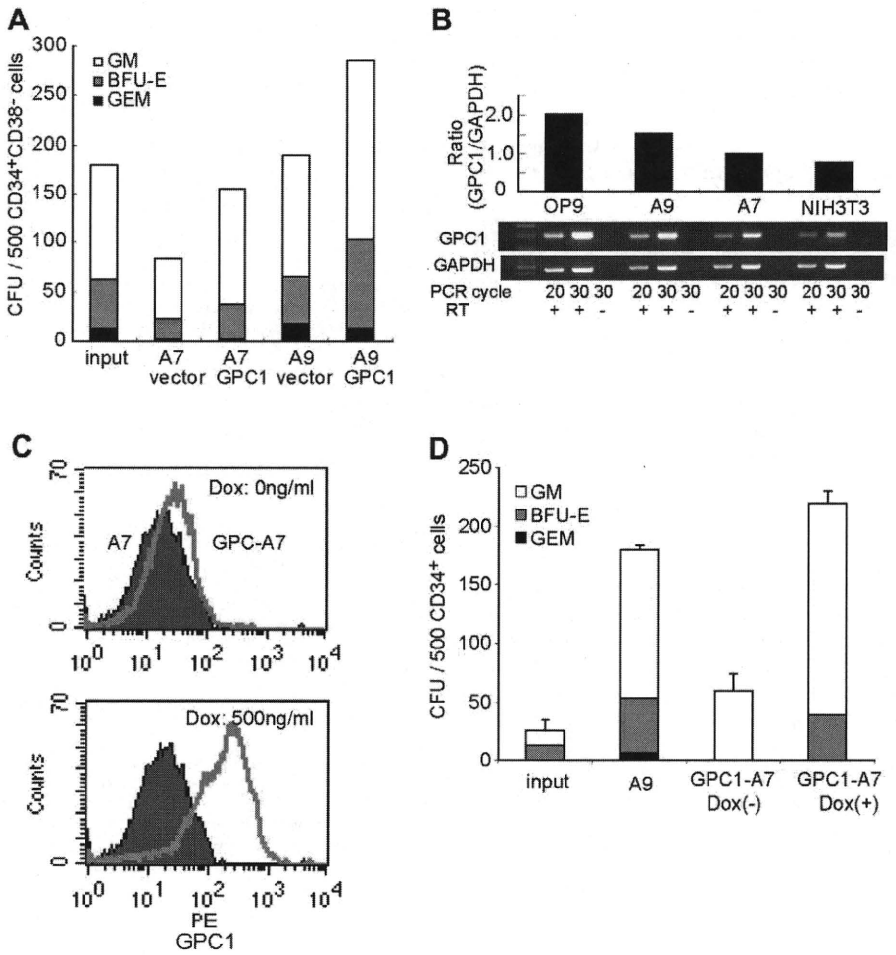

Fig. 3. Hematopoietic supportive activity of Glypican-1. (A) Coculture of Human CB CD34$^+$ CD38- cells with AGM-S3-A9 or AGM-S3-A7 cells that had been retrovirally infected with the GPC-1 expression vector. A total of about 500 human CB CD34$^+$ CD38- cells per well were added to the stromal cells and the cells were cocultured for two weeks. Colonies were counted at day 14. (B) RT-PCR analysis of GPC1 expression on AGM-S3-A9, AGM-S3-A7, OP9, and NIH3T3 cells. (C) Dox-dependent inducible expression of GPC1 protein in the cell population GPC1-A7 as detected by FACS analysis. (D) Coculture of Human CB CD34$^+$ cells with the cell population GPC1-A7. A total of about 500 human CB CD34$^+$ cells per well were cocultured with GPC1-A7 for two weeks in the presence or absence of Dox (500 ng/ml). Colonies were counted at day 14.

to S3-A9 cells (Fig. 3A). Furthermore, the forced expression of GPC1 in AGM-S3-A9 cells enhanced the supporting ability, which means that the supportive activity of AGM-S3-A9 by intrinsic expression of GPC1 is not saturated in those cells and compulsory expression of GPC1 could induce the cells to perform to their full potential. In support of the gene chip assay results, RT-PCR analysis confirmed that AGM-S3-A9 and OP9 cells expressed 1.5 to 2.0 fold more of GPC1 than AGM-S3-A7 (Fig. 3B).

To confirm the ability of GPC1 to support human hematopoiesis, we used the tetracycline (tet)-regulated gene expression system. We established AGM-S3-A7 cells expressing GPC1 (henceforth, GPC1-A7 cells) under the control of a tet-responsive element using the reverse tet-regulated retroviral vector pLRT [23]. The tet-responsive expression of GPC1 was verified by FACS analysis (Fig. 3C). In the absence of Dox, GPC1-A7 cells exhibited little supportive activity and were comparable to the parental AGM-S3-A7 cells. In contrast, in the presence of Dox, GPC1-A7 stimulated the proliferation of HPCs, including BFU-E, in the human $CD34^+$ cells to levels similar to that achieved with S3-A9 cells (Fig. 3D). These results suggest that an increase in the level of expression of GPC1 could restore the ability of AGM-S3-A7 cells to stimulate HPC proliferation. However, it remains unclear how GPC-1 could affect hematopoiesis. In accordance with the fact that GPC1 is known as a co-receptor that facilitates the interaction of growth factors, we found that bFGF and VEGF bind to a soluble form of recombinant human GPC1 protein *in vitro* (data not shown). In the context of those observations, GPC1 may help to coordinate the microenvironment of hematopoiesis by presenting growth factors.

Our experiments have characterized one gene, GPC1, that plays a role in the HSC supporting capacity of AGM-S3-A9. Also, our studies provide important clues to elucidate the molecular mechanisms of a HSC supportive niche in AGM. However, we could not reconstitute a hematopoiesis-supportive microenvironment by only using recombinant proteins without stromal cells. Defining the culture conditions required for expanding LTR-HSCs might be helpful for clinical use. Perhaps combinations of up-regulated genes in AGM-S3-A9 might support hematopoiesis, though further investigation is still needed.

Accession number

Microarray data are accessible through accession number GSE11891, the National Center for Biotechnology Information Gene Expression Omnibus database (http://www.ncbi.nlm.nih.gov/geo).

Acknowledgments

We thank Dr. Nakauchi for providing C57BL/6-Ly5.1 mice, Dr. Kitamura for providing pMXIG vectors and PLAT-E, and Dr. Hagiwara for providing pLRT vectors. We thank Dr. Ralph Kubo for critical reading of the manuscript. We are grateful to Yoko Yamada, Noriko Tawara, Hiromi Shimizu, Naoko Tago and Terumi Yamamoto, for their excellent technical assistance.

Appendix A. Supplementary data

Supplementary data associated with this article can be found, in the online version, at doi:10.1016/j.bbrc.2008.09.123.

References

[1] R. Schofield, The relationship between the spleen colony-forming cell and the haemopoietic stem cell, Blood Cells 4 (1978) 7–25.
[2] M. Ogawa, Differentiation and proliferation of hematopoietic stem cells, Blood 81 (1993) 2844–2853.
[3] E. Fuchs, T. Tumbar, G. Guasch, Socializing with the neighbors: stem cells and their niche, Cell 116 (2004) 769–778.
[4] F. Arai, A. Hirao, M. Ohmura, H. Sato, S. Matsuoka, K. Takubo, K. Ito, G.Y. Koh, T. Suda, Tie2/angiopoietin-1 signaling regulates hematopoietic stem cell quiescence in the bone marrow niche, Cell 118 (2004) 149–161.
[5] P. Gupta, T.R. Oegema Jr., J.J. Brazil, A.Z. Dudek, A. Slungaard, C.M. Verfaillie, Structurally specific heparan sulfates support primitive human hematopoiesis by formation of a multimolecular stem cell niche, Blood 92 (1998) 4641–4651.
[6] D.R. Coombe, S.M. Watt, C.R. Parish, Mac-1 (CD11b/CD18) and CD45 mediate the adhesion of hematopoietic progenitor cells to stromal cell elements via recognition of stromal heparan sulfate, Blood 84 (1994) 739–752.
[7] S.M. Watt, J. Williamson, H. Genevier, J. Fawcett, D.L. Simmons, A. Hatzfeld, S.A. Nesbitt, D.R. Coombe, The heparin binding PECAM-1 adhesion molecule is expressed by $CD34^+$ hematopoietic precursor cells with early myeloid and B-lymphoid cell phenotypes, Blood 82 (1993) 2649–2663.
[8] A.O. Hueber, M. Pierres, H.T. He, Sulfated glycans directly interact with mouse Thy-1 and negatively regulate Thy-1-mediated adhesion of thymocytes to thymic epithelial cells, J. Immunol. 148 (1992) 3692–3699.
[9] A.M. Muller, A. Medvinsky, J. Strouboulis, F. Grosveld, E. Dzierzak, Development of hematopoietic stem cell activity in the mouse embryo, Immunity 1 (1994) 291–301.
[10] A. Medvinsky, E. Dzierzak, Definitive hematopoiesis is autonomously initiated by the AGM region, Cell 86 (1996) 897–906.
[11] M. Takeuchi, T. Sekiguchi, T. Hara, T. Kinoshita, A. Miyajima, Cultivation of aorta-gonad-mesonephros-derived hematopoietic stem cells in the fetal liver microenvironment amplifies long-term repopulating activity and enhances engraftment to the bone marrow, Blood 99 (2002) 1190–1196.
[12] M.J. Xu, K. Tsuji, T. Ueda, Y.S. Mukouyama, T. Hara, F.C. Yang, Y. Ebihara, S. Matsuoka, A. Manabe, A. Kikuchi, M. Ito, A. Miyajima, T. Nakahata, Stimulation of mouse and human primitive hematopoiesis by murine embryonic aorta-gonad-mesonephros-derived stromal cell lines, Blood 92 (1998) 2032–2040.
[13] M. Osawa, K. Hanada, H. Hamada, H. Nakauchi, Long-term lymphohematopoietic reconstitution by a single CD34-low/negative hematopoietic stem cell, Science 273 (1996) 242–245.
[14] M. Osawa, K. Nakamura, N. Nishi, N. Takahasi, Y. Tokuomoto, H. Inoue, H. Nakauchi, In vivo self-renewal of c-Kit+ Sca-1+ Lin(low/-) hemopoietic stem cells, J. Immunol. 156 (1996) 3207–3214.
[15] S. Morita, T. Kojima, T. Kitamura, Plat-E: an efficient and stable system for transient packaging of retroviruses, Gene Ther. 7 (2000) 1063–1066.
[16] H. Kodama, M. Nose, S. Niida, S. Nishikawa, S. Nishikawa, Involvement of the c-kit receptor in the adhesion of hematopoietic stem cells to stromal cells, Exp. Hematol. 22 (1994) 979–984.
[17] K.C. Weisel, Y. Gao, J.H. Shieh, M.A. Moore, Stromal cell lines from the aorta-gonado-mesonephros region are potent supporters of murine and human hematopoiesis, Exp. Hematol. 34 (2006) 1505–1516.
[18] T. Sugiyama, H. Kohara, M. Noda, T. Nagasawa, Maintenance of the hematopoietic stem cell pool by CXCL12-CXCR4 chemokine signaling in bone marrow stromal cell niches, Immunity 25 (2006) 977–988.
[19] H.E. Broxmeyer, L. Kohli, C.H. Kim, Y. Lee, C. Mantel, S. Cooper, G. Hangoc, M. Shaheen, X. Li, D.W. Clapp, Stromal cell-derived factor-1/CXCL12 directly enhances survival/antiapoptosis of myeloid progenitor cells through CXCR4 and G(α)i proteins and enhances engraftment of competitive, repopulating stem cells, J. Leukoc. Biol. 73 (2003) 630–638.
[20] K.M. Zsebo, D.A. Williams, E.N. Geissler, V.C. Broudy, F.H. Martin, H.L. Atkins, R.Y. Hsu, N.C. Birkett, K.H. Okino, D.C. Murdock, et al., Stem cell factor is encoded at the Sl locus of the mouse and is the ligand for the c-kit tyrosine kinase receptor, Cell 63 (1990) 213–224.
[21] E. Huang, K. Nocka, D.R. Beier, T.Y. Chu, J. Buck, H.W. Lahm, D. Wellner, P. Leder, P. Besmer, The hematopoietic growth factor KL is encoded by the Sl locus and is the ligand of the c-kit receptor, the gene product of the W locus, Cell 63 (1990) 225–233.
[22] M. Nishikawa, T. Tahara, A. Hinohara, A. Miyajima, T. Nakahata, A. Shimosaka, Role of the microenvironment of the embryonic aorta-gonad-mesonephros region in hematopoiesis, Ann. NY Acad. Sci. 938 (2001) 109–116.
[23] T. Watsuji, Y. Okamoto, N. Emi, Y. Katsuoka, M. Hagiwara, Controlled gene expression with a reverse tetracycline-regulated retroviral vector (RTRV) system, Biochem. Biophys. Res. Commun. 234 (1997) 769–773.

Downloaded from bjo.bmj.com on 28 July 2008

Association of varicella zoster virus load in the aqueous humor with clinical manifestations of anterior uveitis in herpes zoster ophthalmicus and zoster sine herpete

S Kido,[1] S Sugita,[1] S Horie,[1] M Miyanaga,[2] K Miyata,[2] N Shimizu,[3] T Morio,[4] M Mochizuki[1]

[1] Department of Ophthalmology & Visual Science, Tokyo Medical and Dental University, Tokyo, Japan; [2] Miyata Eye Hospital, Miyakonojyo, Japan; [3] Department of Virology, Medical Research Institute, Tokyo Medical and Dental University, Tokyo, Japan; [4] Center for Cell Therapy, Tokyo Medical and Dental University, Tokyo, Japan

Correspondence to: Dr S Sugita, Department of Ophthalmology & Visual Science, Tokyo Medical and Dental University Graduate School of Medicine, 1-5-45 Yushima, Bunkyo-ku, Tokyo 113-8519, Japan; sunaoph@tmd.ac.jp

Accepted 4 August 2007
Published Online First 1 February 2008

ABSTRACT

Aim: To investigative whether clinical manifestations of anterior uveitis are associated with the viral load of varicella zoster virus (VZV) in the aqueous humor in patients with herpes zoster ophthalmicus (HZO) and zoster sine herpete (ZSH).

Methods: After informed consent was given, an aliquot of aqueous humor was collected from patients with VZV anterior uveitis (n = 8). Genomic DNA of the human herpes viruses was measured in the aqueous humor by two PCR assays: a qualitative multiplex PCR and a quantitative real-time PCR.

Results: All patients had unilateral acute anterior uveitis with high intraocular pressure, mutton fat keratic precipitates with some pigmentation, and trabecular meshwork pigmentation. Multiplex PCR demonstrated VZV genomic DNA in all of the samples, but not in other human herpes virus samples (human simplex virus types 1 and 2, Epstein–Barr virus, cytomegalovirus and human herpes virus types 6, 7 and 8). Real-time PCR revealed a high copy number of VZV DNA in the aqueous humor. After the initial onset of anterior uveitis, iris atrophy and distorted pupil with paralytic mydriasis developed. The intensity of iris atrophy and pupil distortion, but not ocular hypertension, correlated with the viral load of VZV in the aqueous humor.

Conclusion: VZV viral load in the aqueous humor correlated significantly with damage to the iris (iris atrophy and pupil distortion) in patients with HZO and ZSH.

Varicella zoster virus (VZV) affects the first branch of the trigeminal nerve and is known to cause unilateral anterior uveitis (VZV anterior uveitis) characterised by mutton-fat keratic precipitates (KPs), trabecular meshwork pigmentation, ocular hypertension, iris atrophy and distorted pupil. Systemic signs in VZV iridocyclitis can be herpes zoster ophthalmicus (HZO) with skin eruptions or zoster sine herpete (ZSH) without skin eruptions but solely with neuralgia. Using PCR, previous studies have revealed genomic DNA of VZV in the aqueous humor in patients with anterior uveitis with HZO and ZSH.[1 2] Recent advances in molecular biology now make it possible for quantitative measurement of the viral load using real-time PCR. Therefore, this study aimed to quantitatively measure the viral load of VZV in the aqueous humor and analyse the correlation between viral load in the aqueous humor and clinical manifestations of VZV anterior uveitis in patients with HZO and ZSH.

MATERIALS AND METHODS

Subjects

The subjects were eight patients (three men and five women; age range 43–71 years (mean 61)) with diagnosed VZV anterior uveitis at Tokyo Medical and Dental University Hospital and Miyata Hospital between December 1999 and September 2007. The clinical diagnosis of VZV anterior uveitis was based on observation of anterior uveitis associated with either HZO or ZSH. After informed consent had been obtained, an aliquot of aqueous humor (0.1–0.2 ml) was obtained from each patient. The research followed the tenets of the Declaration of Helsinki, and the study was approved by the institutional ethics committees of Tokyo Medical and Dental University.

PCR assay

The aqueous humor samples were centrifuged at 3000 rpm for 5 min and used for the following PCR assays: multiplex PCR and real-time PCR.[3] Multiplex PCR was designed to qualitatively measure the genomic DNA of eight human herpes viruses: herpes simplex virus type 1 (HSV-1) and type 2 (HSV-2), VZV, Epstein–Barr virus (EBV), cytomegalovirus (CMV), human herpes virus type 6 (HHV-6), type 7 (HHV-7) and type 8 (HHV-8). DNA was extracted from the aqueous humor samples using a DNA minikit (Qiagen, Valencia, CA, USA). Multiplex PCR was performed using LightCycler (Roche, Basle, Switzerland). The primer sequences and PCR conditions for VZV were as previously described.[4]

Real-time PCR was performed only for HHV, the genomic DNA of which was detected by multiplex PCR. It was performed by using Amplitaq Gold and a Real-Time PCR 7300 system (ABI, Forster City, CA, USA). The primer sequences for VZV (ORF29) used in real-time PCR were designed to use Primer Express (ABI): forward, AACTTTTACATCCAGCCTGGCG; reverse, GAAAACCCAAACCGTTCTCGAG. The probe was FAM-TGTCTTTCACGGAGGCAAAC-ACGT-TAMRA. The following PCR conditions were used: denaturation at 95°C for 10 min, 95°C for 15 s, and 60°C for 60 s for 40 cycles.

Downloaded from bjo.bmj.com on 28 July 2008

Table 1 Clinical findings at initial presentation in patients with varicella zoster virus (VZV) anterior uveitis

Case	Age (years)	Sex	Eye	Initial ocular findings: VA	IOP (mm Hg)	Mutton-fat KPs	Cells in AC	Flare in AC	Pigmentation in the AC angle	Eruption	Time from onset to treatment	Herpes virus DNA: VZV	Others*
1	67	F	Left	0.3	38	+	3+	271	Wide	–	2 months	+	–
2	70	F	Left	0.3	22	+	3+	106	Partial	+	2 weeks	+	–
3	68	F	Right	0.8	10	+	2+	34	None	–	2 months	+	–
4	56	M	Left	1.2	46	+	3+	241	Partial	+	2 months	+	–
5	70	F	Left	1.2	25	–	1+	13	Partial	–	2 months	+	–
6	44	M	Right	0.6	46	–	3+	140	Partial	+	1 week	+	–
7	43	F	Left	1.2	28	–	2+	15	Partial	–	1 month	+	–
8	71	M	Right	0.3	28	–	2+	13	None	+	None	+	–

Aqueous humor samples from eight cases were analysed for human herpes virus DNA by multiplex PCR.
*Herpes viruses excluding VZV, ie, herpes simplex virus type 1 and type 2, Epstein–Barr virus, cytomegalovirus, human herpes virus types 6, 7 and 8.
VA, visual acuity; IOP, intraocular pressure; KPs, keratic precipitates; AC, anterior chamber.

Statistical analysis

Statistical analysis was performed using the Mann–Whitney U test. Statistical significance was set at $p<0.05$.

RESULTS

Clinical manifestations

In four of the patients, there was an episode of skin eruption with neuralgia in the area of the first branch of the trigeminal nerve; this was clinically diagnosed as HZO (table 1). No skin eruptions were observed in the other patients, although they complained of pain near the first branch of the trigeminal nerve, leading to the diagnosis of ZSH. At various intervals after the onset of HZO or ZSH, the patients developed unilateral anterior uveitis. All patients had cells and flare in the anterior chamber, with increased flare values measured by a laser flare meter (Cowa, Tokyo, Japan). Four patients exhibited mutton-fat KPs (table 1), which had brownish pigmentation and were small or medium in size. Three patients with HZO already exhibited iris atrophy and pupil distortion on referral. High intraocular pressure (IOP) was recorded in all patients except in case 3 (table 1). A gonioscopic examination revealed wide, open angles in all patients, and higher pigmentation in the affected eye than the other eye in six of the eight patients. Ophthalmoscopic examinations revealed no significant inflammatory lesions in the retina and choroid. These clinical results led us to a diagnosis of anterior uveitis associated with HZO or ZSH, with paracentesis subsequently performed in order to carry out the PCR analysis.

After confirmation of the presence of VZV in the aqueous humor by multiplex PCR, systemic anti-VZV agents (aciclovir or valaciclovir) and aciclovir ointment were administered for at least 4 weeks together with a topical corticosteroid (eg, betamethasone) and anti-glaucoma agents (eg, timolol and latanoprost). Iris atrophy and pupil distortion developed during the clinical course (fig 1, table 2). The anterior uveitis and high IOP responded well to treatment.

PCR analysis of the aqueous humor

Qualitative PCR (multiplex PCR) detected genomic DNA of VZV but not of other human herpes viruses (HSV-1, HSV-2, EBV, CMV, HHV-6, HHV-7 and HHV-8) in the aqueous humor of all eight patients (table 1). In peripheral blood samples, however, no genomic DNA of any of the eight human herpes viruses, including VZV, was detected in any of the patients.

Quantitative PCR (real-time PCR) detected significant viral loads of VZV DNA in the aqueous humor of the eight patients ranging from 3.8×10^2 to 1.2×10^7 copies/ml (table 2). It is of note that the VZV viral load in the aqueous humor correlated with the intensity of iris atrophy and pupil distortion (table 2, fig 1). Patient 1 had the highest VZV viral load (1.2×10^7 copies/ml) in the aqueous humor and also had the most severe iris atrophy, with multiple wide areas of segmental iris atrophy and a widely dilated pupil (fig 1A, table 2). Patients 2–5 had the second

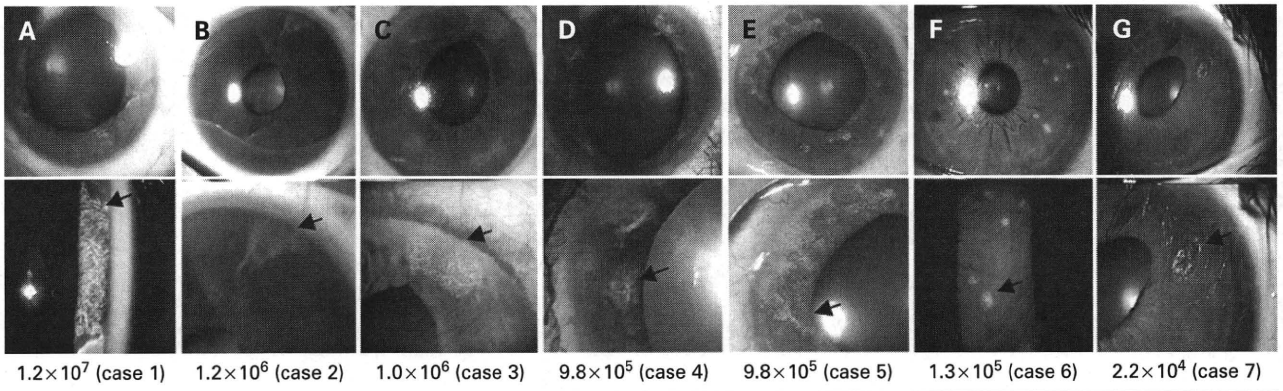

Figure 1 Iris photographs for patients with varicella zoster virus (VZV) anterior uveitis. Slit-lamp photographs are available for seven cases as shown. The numbers indicate the copies of the VZV genomic DNA for each of the aqueous humor samples (copies/ml). Arrows point to areas of iris atrophy. Consent has been obtained for publication of this figure.

Downloaded from bjo.bmj.com on 28 July 2008

Table 2 Virological analysis and ocular findings after treatment of patients with varicella zoster virus (VZV) anterior uveitis

Case	VZV DNA (copies/ml)	Final ocular findings: VA	IOP (mm Hg)	Cells in AC	Flare in AC	Iris atrophy	Extent of iris atrophy (%)	Pupil	Maximum pupil diameter (mm)	Systemic treatment	Follow-up (months)
1	1.2×10^7	mm	10	–	13	Wide	40	Distorted, mydriasis	8.1	ACV, ACZ	48
2	1.2×10^6	0.9	14	–	8	Segmental	4	Distorted, mild mydriasis	3.4	VCV, ACZ	5
3	1.0×10^6	0.8	7	–	5	Segmental	15	Distorted, mydriasis	5.0	VCV	4
4	9.8×10^5	0.9	10	–	73	Segmental	20	Distorted, mydriasis	7.9	VCV	12
5	9.8×10^5	0.8	20	–	22	Segmental	29	Distorted, mydriasis	7.0	VCV	5
6	1.3×10^5	1.5	13	–	6	Circular	1	Normal	2.6	ACV	26
7	2.2×10^4	2	16	–	3	Circular	1	Distorted, mild mydriasis	4.3	VCV	13
8	3.8×10^2	1.2	12	–	9	None	0	Normal	2.6	ACV, ACZ	4

The copy number of the VZV genome in aqueous humor was evaluated with real-time PCR. The extent of iris atrophy was calculated using Photoshop Elements V2.0. ACV, aciclovir; ACZ, acetazolamide; mm, motus manus; VCV, valaciclovir.

highest viral loads in the aqueous humor (~1×10^6 copies/ml), and these patients developed multiple segmental or circular iris atrophy with moderate pupil distortion, although these signs were not as marked as in patient 1 (fig 1B–E, table 2). Patients 6 and 7 had the third highest viral load (10^5–10^4 copies/ml) and exhibited circular iris atrophy with minimum pupil distortion (fig 1F,G). Patient 8 had the lowest viral load. This patient exhibited no iris atrophy and the pupil remained normal throughout the clinical course.

We next examined whether higher viral load in the aqueous humor was significantly associated with the intensity of the iris atrophy and pupil distortion. For this analysis, we separated the patients into two groups: higher viral load (patients 1–5) and lower viral load (patients 6–8). The extent of iris atrophy was significantly ($p<0.05$) larger in the group with higher viral load. In addition, the maximum pupil diameter in the pupil distortion was significantly ($p<0.05$) larger in the group with higher viral load. These results suggest that higher viral load in the aqueous humor is closely associated with the intensity of the iris atrophy and pupil distortion.

DISCUSSION

Human herpes viruses are known to be involved in many ocular pathological conditions, such as keratitis, anterior uveitis and necrotising retinitis. Early treatment with anti-viral agents, based on a rapid and accurate diagnosis of the viral infection in ocular tissues, is clinically important in order to avoid the irreversible tissue damage and visual impairment caused by viral infection. Recent advances in PCR methodology have made it possible to screen for viral infection and further quantify the intensity of the viral infection in ocular inflammatory diseases.[1–3 5–8] Asano *et al*[8] detected herpes virus DNA (VZV or HSV-2) in three cases of acute retinal necrosis using real-time PCR. They monitored viral load in ocular samples of these patients and examined correlations with disease activities of acute retinal necrosis. In this study, we used multiplex PCR to screen for HHV infections (HHV1–8) and real-time PCR to quantify viral load in the aqueous humor of patients with HZO or ZSH.

With multiplex PCR, genomic DNA of VZV was detected in the aqueous humor of all eight patients with HZO and ZSH, and significant VZV viral loads were quantified in the same samples with real-time PCR. After cutaneous lesions or neuralgia, all eight patients with HZO or ZSH developed anterior uveitis, which was characterised by unilateral acute anterior uveitis with high IOP, mutton-fat KPs, trabecular meshwork pigmentation, iris atrophy and pupil distortion, although there were no significant pathological lesions in the cornea or ocular fundus of any of the patients. It is well established that these ocular signs are typical of HZO. The present multiplex PCR data clearly confirm that VZV, but not the other human herpes viruses, is responsible for the anterior uveitis. Furthermore, an important finding in our study was that the extent of iris atrophy and pupil distortion also correlated with the viral load of VZV in the aqueous humor in patients with HZO and ZSH. Unlike iris atrophy, IOP did not correlate with the viral load in the aqueous humor. All but one of the patients had raised IOP ranging from 22 to 46 mm Hg at the onset of anterior uveitis.

This study did not reveal any pathological mechanisms for the correlation of the high VZV viral load with the iris atrophy. However, a previous immunohistological report detected VZV antigens in the stroma and vascular endothelial cells of the iris in anterior uveitis patients with HZO.[9] Another study that used angiography in a patient with HZO showed that there was occlusion of the blood vessels of the atrophic iris.[10] On the basis of previous studies and our present data, we hypothesise that the pathological changes caused by VZV may induce occlusion of the iris vessel leading to iris muscle paralysis, with a net result of iris atrophy and pupil distortion. The higher the viral load in the anterior chamber, the more VZVs there will be in the iris, and thus the more intense the pathological tissue damage.

Early initiation of systemic anti-viral agents, as guided by PCR analysis, would help to avoid, or at least minimise, tissue damage in the iris. Some patients with HZO were only given 1-week systemic anti-viral treatments after the onset of the skin lesions. In these patients, the viral loads of VZV in the aqueous humor were high, and various degrees of iris atrophy and distorted pupil were seen over time. These observations suggest that systemic anti-viral treatments after the onset of HZO are helpful in avoiding or minimising irreversible ocular complications and that qualitative and quantitative PCR can also provide useful information for developing treatments for such patients.

Acknowledgements: We thank Drs Ken Watanabe and Miki Mizukami for technical assistance. This work was supported by a Grant-in-Aid for Young Scientists (B) 18791263 from the Ministry of Education, Culture, Sports, Science and Technology, Japan.

Competing interests: None declared.

Ethics approval: Ethics approval was obtained.

Patient consent: Consent has been obtained for publication of fig 1.

REFERENCES

1. **Yamamoto S,** Tada R, Shimomura Y, *et al*. Detecting varicella-zoster virus DNA in iridocyclitis using polymerase chain reaction. *Arch Ophthalmol* 1995;**113**:1358–9.
2. **Nakamura N,** Tanabe M, Yamada Y, *et al*. Zoster sine herpete with bilateral ocular involvement. *Am J Ophthalmol* 2000;**129**:809–10.

Downloaded from bjo.bmj.com on 28 July 2008

3. **Sugita S,** Shimizu N, Kawaguchi T, *et al*. Identification of human herpesvirus 6 in a patient with severe unilateral panuveitis. *Arch Ophthalmol* 2007**125**:1426–7.
4. **Espy MJ,** Teo R, Ross TK, *et al*. Diagnosis of varicella-zoster virus infections in the clinical laboratory by LightCycler PCR. *J Clin Microbiol* 2000;**38**:3187–9.
5. **De Schryver I,** Rozenberg N, Cassous S, *et al*. Diagnosis and treatment of cytomegalovirus iridocyclitis without retinal necrosis. *Br J Ophthalmol* 2006;**90**:852–5.
6. **Koizumi N,** Yamasaki K, Kawasaki S, *et al*. Cytomegalovirus in aqueous humor from an eye with corneal endotheliitis. *Am J Ophthalmol* 2006;**141**:564–5.
7. **Tran TH,** Rozenberg F, Cassoux N, *et al*. Polymerase chain reaction analysis of aqueous humor samples in necrotising retinitis. *Br J Ophthalmol* 2003;**87**:79–83.
8. **Asano S,** Yoshikawa T, Kimura H, *et al*. Monitoring herpesvirus DNA in three cases of acute retinal necrosis by real-time PCR. *J Clin Virol* 2004;**29**:206–9.
9. **Nakashizuka H,** Yamazaki Y, Tokumaru M, *et al*. Varicella-zoster viral antigen identified in iridocyclitis patient. *Jpn J Ophthalmol* 2002;**46**:70–3.
10. **Marsh RJ,** Easty DL, Jones BR, *et al*. Iritis and iris atrophy in herpes zoster ophthalmicus. *Am J Ophthalmol* 1974;**78**:255–61.

FUNDING AVAILABLE FOR RESEARCH PROJECTS

The Committee on Publication Ethics (COPE) has established a Grant Scheme to fund research in the field of publication ethics. The Scheme is designed to provide financial support to any member of COPE for a defined research project that is in the broad area of the organisation's interests, and specifically in the area of ethical standards and practice in biomedical publishing. The project should have a specific goal and be intended to form the kernel of a future publication.

A maximum sum of £5000 will be allocated to any one project, but applications for smaller sums are welcomed.

The terms and conditions of the Grant are as follows:

- At least one of the applicants must be a member of COPE.
- Calls for applications will be made twice a year with closing dates of 1 December and 1 June. An electronic version of the application form must be sent to the Administrator no later than 12 pm (noon GMT) on the closing date for consideration by COPE Council.
- The application must contain a lay summary of the project, a definition of the question to be posed, sufficient methodological detail to allow assessment of the viability of the project, a clear timeline and a definition of the likely deliverables. A full justification for the sum requested must accompany the application.
- A report on the progress of the research should be presented within one year of the award and at the end of the project. The grant must be used within two years from the date of award, and balance sheets must be forwarded annually. These should be sent to the Administrator. Any remaining funds after two years must be returned.
- It is anticipated that the work stemming from the project will be presented at one of COPE's annual seminar meetings within 2–3 years of the award. Such data may also be published in peer-reviewed journals. Any publications or related presentations at meetings by the recipient emanating in part or whole from COPE's support should be duly acknowledged and copies sent to the Administrator.

Applications are reviewed by a COPE sub-committee. Applicants will be advised of a decision as soon as practicable after the deadline date.

An application form can be obtained by contacting Linda Gough, COPE administrator, at LGough@bmj.com or 020 7383 6602. For more information on COPE, see http://www.publicationethics.org.uk/

The closing date for receipt of applications is 1 December 2007 or 1 June 2008.

Br J Ophthalmol 2008;**92**:505–508. doi:10.1136/bjo.2007.125773

Downloaded from bjo.bmj.com on 28 July 2008

Use of multiplex PCR and real-time PCR to detect human herpes virus genome in ocular fluids of patients with uveitis

S Sugita, N Shimizu, K Watanabe, M Mizukami, T Morio, Y Sugamoto and M Mochizuki

Br. J. Ophthalmol. 2008;92;928-932; originally published online 11 Apr 2008; doi:10.1136/bjo.2007.133967

Updated information and services can be found at:
http://bjo.bmj.com/cgi/content/full/92/7/928

These include:

References This article cites 18 articles, 6 of which can be accessed free at:
http://bjo.bmj.com/cgi/content/full/92/7/928#BIBL

Open Access This article is free to access

Rapid responses You can respond to this article at:
http://bjo.bmj.com/cgi/eletter-submit/92/7/928

Email alerting service Receive free email alerts when new articles cite this article - sign up in the box at the top right corner of the article

Topic collections Articles on similar topics can be found in the following collections

Unlocked (114 articles)
Editor's choice (328 articles)

Notes

To order reprints of this article go to:
http://journals.bmj.com/cgi/reprintform

To subscribe to *British Journal of Ophthalmology* go to:
http://journals.bmj.com/subscriptions/

Downloaded from bjo.bmj.com on 28 July 2008

EDITOR'S CHOICE

Use of multiplex PCR and real-time PCR to detect human herpes virus genome in ocular fluids of patients with uveitis

S Sugita,[1] N Shimizu,[2] K Watanabe,[2] M Mizukami,[3] T Morio,[3] Y Sugamoto,[1] M Mochizuki[1]

[1] Department of Ophthalmology & Visual Science, Medical Research Institute, Tokyo Medical and Dental University, Tokyo, Japan; [2] Department of Virology, Medical Research Institute, Tokyo Medical and Dental University, Tokyo, Japan; [3] Center for Cell Therapy, Tokyo Medical and Dental University, Tokyo, Japan

Correspondence to: Professor M Mochizuki, Department of Ophthalmology & Visual Science, Tokyo Medical and Dental University Graduate School of Medicine, 1-5-45 Yushima, Bunkyo-ku, Tokyo 113-8519, Japan; m.manabu.oph@tmd.ac.jp

Accepted 17 February 2008
Published Online First 11 April 2008

ABSTRACT

Aim: To measure the genomic DNA of human herpes viruses (HHV) in the ocular fluids and to analyse the clinical relevance of HHV in uveitis.

Methods: After informed consent was obtained, a total of 111 ocular fluid samples (68 aqueous humour and 43 vitreous fluid samples) were collected from 100 patients with uveitis. The samples were assayed for HHV-DNA (HHV1–8) by using two different polymerase chain reaction (PCR) assays, qualitative PCR (multiplex PCR) and quantitative PCR (real-time PCR).

Results: In all of the patients with acute retinal necrosis (n = 16) that were tested, either the HSV1 (n = 2), HSV2 (n = 3), or VZV (n = 11) genome was detected. In all patients, high copy numbers of the viral DNA were also noted, indicating the presence of viral replication. In another 10 patients with anterior uveitis with iris atrophy, the VZV genome was detected. When using multiplex PCR, EBV-DNA was detected in 19 of 111 samples (17%). However, real-time PCR analysis of EBV-DNA indicated that there were only six of the 19 samples that had significantly high copy numbers. The cytomegalovirus (CMV) genome was detected in three patients with anterior uveitis of immunocompetent patients and in one immunocompromised CMV retinitis patient. In addition, one patient with severe unilateral panuveitis had a high copy number of HHV6-DNA. There was no HHV7- or HHV8-DNA detected in any of the samples.

Conclusions: A qualitative multiplex PCR is useful in the screening of viral infections. However, the clinical relevance of the virus infection needs to be evaluated by quantitative real-time PCR.

Human herpes virus (HHV) affects various ocular tissues and is known to cause anterior and/or posterior uveitis, which is characterised by mutton-fat keratic precipitates (KPs), ocular hypertension, iris atrophy, vitreous opacity, and necrotic retinitis. Using polymerase chain reaction (PCR), previous studies have demonstrated the presence of genomic DNA for HHV in the aqueous humour and vitreous fluids in patients with herpetic uveitis, including herpetic keratouveitis, herpes zoster ophthalmicus, zoster sine herpete, acute retinal necrosis, and cytomegalovirus retinitis.[1–7] With recent advances in molecular biology, use of real-time PCR now makes it possible for quantitative measurements of the viral load associated with herpes virus diseases in the eye.[5 6] In addition, multiplex qualitative PCR has the advantage of combining several different primer pairs in the same amplification reaction with the net result of producing different specific virus-amplicons in ocular infectious diseases.[7] Therefore, multiplex PCR can be used to detect the presence of viruses within samples.

In this study, we collected ocular samples from various uveitis patients and then tried to detect the HHV genome when using combinations of two PCR systems: (1) multiplex qualitative PCR and (2) real-time quantitative PCR.

MATERIAL AND METHODS

Subjects

Samples of aqueous humour (n = 68) and vitreous fluid (n = 43) were collected from 100 patients with uveitis and ocular lymphoma. Underlying pathology comprised herpetic keratouveitis (n = 7), herpetic anterior uveitis/iridocyclitis (n = 16), acute retinal necrosis (ARN; n = 16), cytomegalovirus (CMV) retinitis (n = 1), human T lymphotropic virus type 1 (HTLV-1) uveitis (n = 1), ocular toxoplasmosis (n = 2), scleritis (n = 3), ocular sarcoidosis (n = 7), Vogt–Koyanagi–Harada (VKH) disease (n = 2), Behçet disease (n = 2), idiopathic uveitis (n = 26) and intraocular lymphoma (n = 12). At the time of sampling, uveitis patients displayed active intraocular inflammation.

An aliquot of 0.1 ml of the aqueous humour was aspirated with a 30 G needle. In patients with uveitis who were undergoing vitreous surgery, non-diluted vitreous fluid samples were collected from the patients during surgery (diagnostic pars-plana vitrectomy). The samples used in this study were collected between 1999 and 2007.

Polymerase chain reaction

Genomic DNA of HHV in the aqueous humour and vitreous fluids was measured through the use of two independent PCR assays: (1) a qualitative multiplex PCR and (2) a quantitative real-time PCR. The result analysis for the PCR is shown in fig 1.

DNA was extracted from samples using an E21 virus minikit (Qiagen, Valencia, CA) installed on a Robotic workstation for automated purification of nucleic acids (BioRobot E21, Qiagen). The multiplex PCR was designed to qualitatively measure genomic DNA of eight human herpes viruses, that is, herpes simplex virus type 1 (HSV-1), type 2 (HSV-2), Varicella-zoster virus (VZV), Epstein–Barr virus (EBV), cytomegalovirus (CMV), human herpes virus type 6 (HHV6), type 7 (HHV7) and type 8 (HHV8). The PCR was performed using a

UNLOCKED

This paper is freely available online under the BMJ Journals unlocked scheme, see http://bjo.bmj.com/info/unlocked.dtl

Downloaded from bjo.bmj.com on 28 July 2008

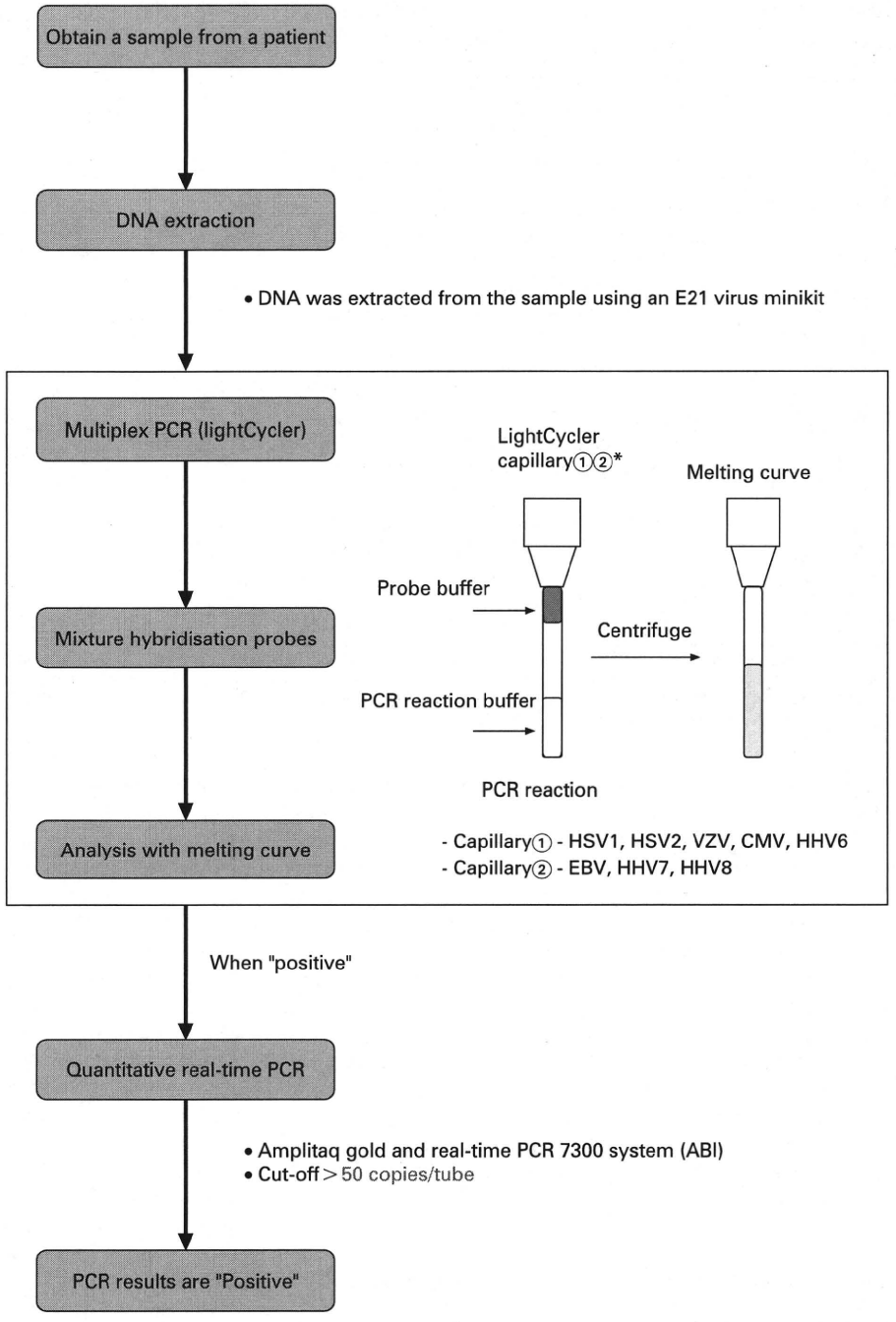

Figure 1 Use of multiplex PCR and real-time PCR for the analysis of human herpes virus family genomic DNA in ocular fluids of patients with uveitis. We performed independent PCR methods to detect herpes viruses, using both a qualitative multiplex PCR and a quantitative real-time PCR. After DNA extraction from each of the samples, multiplex PCR was performed to screen from HHV1 to HHV8 using two LightCycler capillaries. When a "positive" result was observed, real-time PCR was performed to measure the viral load. When more than 50 copies/tube (5×10^3/ml) were observed, the value was considered to be significant. CMV, cytomegalovirus; EBV, Epstein–Barr virus; HHV, human herpes virus; HSV, herpes simplex virus; VZV, Varicella-zoster virus.

LightCycler (Roche, Switzerland). Primers and probes of HHV1–8 and the PCR conditions have been described previously.[8] Specific primers for the virus were used with Accuprime Taq (Invitrogen, Carlsbad, CA). Products were subjected to 40 cycles of PCR amplification. Hybridisation probes were then mixed with the PCR products. Subsequently, real-time PCR was performed only for the human herpes virus, with the genomic DNA detected by multiplex PCR (fig 1). The real-time PCR was performed using Amplitaq Gold and the Real-Time PCR 7300 system (ABI, Foster City, CA). The sequence of the HHV1–8 primers and probes are shown in table 1. The primers of the viruses and the PCR conditions have been described in previous reports.[9–13] Our research group has also previously reported the primers of the sequences for VZV.[14] All of the products obtained were subjected to 45 cycles of PCR amplification. The value of viral copy number in the sample was considered to be significant, when more than 50 copies/tube (5×10^3/ml) were observed.

RESULTS

Our initial PCR results indicated HHV positivity in the ocular fluids of uveitis patients. As shown in table 2, multiplex PCR detected seven patients with HSV1-DNA while real-time PCR found that all seven of these patients also had a high HSV1 viral load. In addition, HSV2-DNA was detected in three patients, with all of these patients having a high viral load. In 29 patients,

Downloaded from bjo.bmj.com on 28 July 2008

Table 1 Sequence for primers and probes in human herpes viruses (HHV) using real-time PCR

Herpes virus	Sequence for primers and probes	Amplification
HSV1 and 2	HSV-F: CGCATCAAGACCACCTCCTC	gB
	HSV-R: GCTCGCACCACGCGA	
	HSV1-P: JOE-TGGCAACGCGGCCCAAC-TAMRA	
	HSV2-P: FAM-CGGCGATGCGCCCCAG-TAMRA	
VZV	VZV-F: AACTTTTACATCCAGCCTGGCG	ORF29
	VZV-R: GAAAACCCAAACCGTTCTCGAG	
	VZV-P: FAM-TGTCTTTCACGGAGGCAAACACGT-TAMRA	
EBV	EBV-F: CGGAAGCCCTCTGGACTTC	BALF5
	EBV-R: CCCTGTTTATCCGATGGAATG	
	EBV-P: FAM-TGTACACGCACGAGAAATGCGCC-TAMRA	
CMV	CMV-F: CATGAAGGTCTTTGCCCAGTAC	IE-1
	CMV-R: GGCCAAAGTGTAGGCTACAATAG	
	CMV-P: FAM-TGGCCCGTAGGTCATCCACACTAGG-TAMRA	
HHV6	HHV6-F: GACAATCACATGCCTGGATAATG	U65-U66
	HHV6-R: TGTAAGCGTGTGGTAATGTACTAA	
	HHV6-P: FAM-AGCAGCTGGCGAAAAGTGCTGTGC-TAMRA	
HHV7	HHV7-F: CGGAAGTCACTGGAGTAATGACAA	U37
	HHV7-R: CCAATCCTTCCGAAACCGAT	
	HHV7-P: FAM-CTCGCAGATTGCTTGTTGGCCATG-TAMRA	
HHV8	HHV8-F: CCTCTGGTCCCCATTCATTG	ORF65
	HHV8-R: CGTTTCCGTCGTGGATGAG	
	HHV8-P: FAM-CCGGCGTCAGACATTCTCACAACC-TAMRA	

The real-time herpes simplex virus (HSV) PCR is a multiplexing PCR that can detect both HSV1 and HSV2 DNA in the same reaction. The optimised gB primer pairs amplify both HSV1 and 2 with equal efficiency, with the two type-specific probes labelled with different fluorescent dyes. HSV1 probe is labelled with JOE at the 5′-end and with TAMRA at the 3′-end. HSV2 probe is labelled with FAM at the 5′-end and with TAMRA at the 3′-end.
CMV, cytomegalovirus; EBV, Epstein–Barr virus; VZV, Varicella-zoster virus.

VZV-DNA was detected, but only 21 patients (72%) had a high viral load. EBV was detected in 19 patients, but only six out of the 19 cases were positive (32%). CMV-DNA was detected in six patients, with four out of the six cases (67%) found to be positive by the real-time PCR. HHV6-DNA was detected in only one patient by both of the PCR methods. There were no patients for which HHV7 and HHV8 were detected. Overall, there were 65 multiplex PCR positive patients and 42 real-time PCR positive patients (table 2). Clinically, we decided that only if HHV-DNA could be detected in a sample (aqueous humour and/or vitreous) by both PCR methods would the patient then be considered to be positive. If a patient was found to be positive by only one of the PCR methods, for example, positive by multiplex qualitative PCR and negative (<50 copies/tube) by real-time quantitative PCR, we did not take this as PCR-positive (fig 1).

Table 2 Human herpes virus-PCR positivity in ocular fluids of 100 patients with uveitis

Herpes virus	Multiplex PCR	Real-time PCR
HSV1	7/100 (7%)	7/7 (100%)
HSV2	3/100 (3%)	3/3 (100%)
VZV	29/100 (29%)	21/29 (72%)
EBV	19/100 (19%)	6/19 (32%)
CMV	6/100 (6%)	4/6 (67%)
HHV6	1/100 (1%)	1/1 (100%)
HHV7	0/100 (0%)	–
HHV8	0/100 (0%)	–
Total	65/100 (65%)	42/65 (65%)

Qualitative multiplex PCR was performed in order to screen for and detect human herpes virus (HHV) genomic DNA, HHV1–HHV8. When the genomic DNA was detected by the multiplex PCR (n = 65), real-time PCR was then performed only for the HHV.
CMV, cytomegalovirus; EBV, Epstein–Barr virus; HSV, herpes simplex virus; VZV, Varicella-zoster virus.

Subsequently, we analysed the results for each the viruses, from HHV1 to HHV8. The summary of the results is shown in table 3. HSV1 was detected in two cases of keratouveitis, and in three cases of anterior uveitis. These patients had mutton-fat KPs, ocular hypertension and anterior chamber cells. HSV1 was also detected in two cases of acute retinal necrosis (ARN). HSV2 was detected in three cases of ARN. VZV was detected in 10 cases of herpetic anterior uveitis and in 11 cases of ARN. During the time after the initial onset of anterior uveitis, iris atrophy developed in these patients. Higher viral load in the aqueous humour was well correlated with tissue damage, such as iris atrophy.[14] In addition, as we have reported previously, real-time PCR of the ocular fluids from ARN patients (n = 16) indicated high viral loads of VZV (n = 11, 69%), HSV1 (n = 2, 12%), and HSV2 (n = 3, 19%).[8]

EBV was detected in only one case of idiopathic uveitis. This patient had acute anterior uveitis with hypopyon and was HLA-B27 negative. Therefore, as previously reported, we diagnosed EBV-related acute anterior uveitis.[15] EBV was also detected in two cases of VZV-associated anterior uveitis and in two cases of VZV-ARN. This suggests that these patients have a high copy number of VZV, as well as EBV in their ocular fluids. EBV was also detected in one case of ocular B-cell lymphoma.

CMV was detected in a case of cytomegalovirus retinitis and in three cases of CMV-associated anterior uveitis. Representative results from the multiplex qualitative PCR can be seen in fig 2. CMV-DNA was detected in the aqueous humour, and quantitative real-time PCR revealed there were 2.3×10^5 copies/mL of CMV-DNA in the specimen. As we previously reported, in the affected eye there were whitish small-size mutton-fat KPs along with mild inflammation in the anterior chamber.[16] During the 8 years this particular patient was followed, he had been considered to have a case of Posner–Schlossman syndrome. This patient had no retinitis, and additionally he was not found to be immunocompromised.

Br J Ophthalmol 2008;**92**:928–932. doi:10.1136/bjo.2007.133967

Downloaded from bjo.bmj.com on 28 July 2008

Table 3 PCR results for each herpes virus genome in patients with uveitis

Herpes virus	Clinical diagnosis	PCR-positive*/total no of patients
HSV1	Herpetic keratouveitis	2/7†
	Herpetic anterior uveitis	3/16
	Acute retinal necrosis	2/16
	Others	0/61
HSV2	Acute retinal necrosis	3/16
	Others	0/84
VZV	Herpetic anterior uveitis	10/16
	Acute retinal necrosis	11/16
	Others	0/68
EBV	Idiopathic uveitis	1/26
	Herpetic anterior uveitis (VZV)	2/16
	Acute retinal necrosis (VZV)	2/16
	Intraocular lymphoma	1/12
	Others	0/30
CMV	Herpetic anterior uveitis	3/16
	Cytomegalovirus retinitis	1/1
	Others	0/83
HHV6	Idiopathic uveitis	1/26
	Others	0/74
HHV7	–	0/100
HHV8	–	0/100

*Detection of HHV-DNA by both multiplex PCR and real-time PCR.
†In the seven patients with keratouveitis, our PCR system detected HSV1-DNA in two patients.
CMV, cytomegalovirus; EBV, Epstein–Barr virus; HHV, human herpes virus; HSV, herpes simplex virus; VZV, Varicella-zoster virus.

A high copy number of HHV6-DNA was detected in only one patient with severe unilateral panuveitis. In this patient, multiple retinal exudates, vitreous opacity, along with a whitish mass lesion were observed in the affected eye. We reported this case as HHV6-associated panuveitis.[17] In the current study, HHV7- or HHV8-DNA was not detected in any of the patients (table 3).

DISCUSSION

Human herpes viruses (HHV) can widely affect the eye and be expressed in ocular tissues or excreted in ocular fluids. Previously, the diagnosis of intraocular HHV infection was made by measuring local production of specific anti-virus antibodies—for example, using the Goldmann–Witmer coefficient. Recently, diagnosis has also been performed through the detection of the virus genome by PCR. Cell-free herpes virus DNA has been detected in the aqueous humour and vitreous fluids of patients with uveitis.[1–7] In the current study, we showed that intraocular HHV-DNA was detectable over a wide range of HHV-associated uveitis when analysis was performed using the two PCR methods. Thus, the current PCR system may be a valuable tool in the diagnosis of infectious uveitis. In addition, with the use of these examinations, this allows non-herpetic uveitis patients to be excluded.

When faced with a clinical situation that suggests a differential diagnosis of HHV1–8, the multiplex PCR assay can provide a rapid and reliable diagnosis, even when only small sample amounts are available for examination in the ocular microbiology laboratory. The majority of the viruses associated with eye diseases are related to the herpes virus group. Therefore, the last decade has seen several studies concluding that herpes virus PCR-based laboratory investigations are valuable tools in the diagnosis of viral diseases of the eye. The advantages of developing the multiplex PCR assay are obvious,

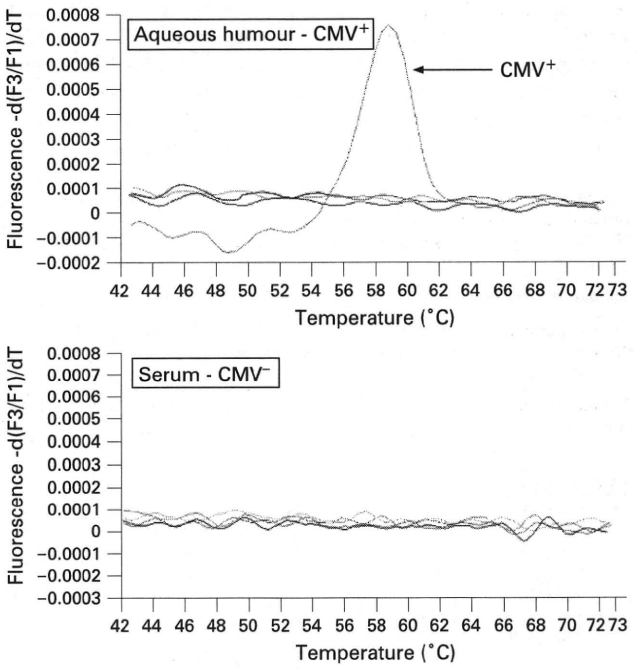

Figure 2 Results for a multiplex PCR in a patient with anterior uveitis. At 58°C, a significant positive curve was seen, indicating the detection of cytomegalovirus (CMV) genomic DNA in the aqueous humour. The other herpes viruses, such as herpes simplex virus (HSV) 1, HSV2, Varicella-zoster virus, Epstein–Barr virus, human herpes virus (HHV6), HHV7 and HHV8, were found to be negative in this particular sample. In addition, CMV-DNA was not detected in the patient's serum.

with several of them reported as being useful in the detection of herpes viruses when various combinations are employed.[7 18 19] In the current study, we were able to rapidly screen for the detection of the virus genome of all eight types of human herpes viruses by using several different primer pairs. When positive results were noted, we then used real-time quantitative PCR to examine the viral load using different primer pairs. This allowed us to confirm our positive results through the use of two PCR combinations.

It is important to discuss the significance of the high viral load of HHV in these patients. The finding of high viral loads in the ocular fluids indicates that virus replication takes place in the eye, suggesting a direct pathogenic role in intraocular inflammation. In the current study, some patients had previously been on systemic or topical corticosteroids over long periods of times before we collected the ocular samples. Therefore, we have to consider that long-term usage of topical and/or systemic steroids might be responsible for the creation of a steroid reservoir that could lead to a localised immunosuppressed state, thereby resulting in HHV replication. In order to be able to avoid the irreversible tissue damage and visual impairment caused by the viral infection, early treatment with anti-viral agents is clinically important, and this can be achieved if there is a rapid and accurate diagnosis of the viral infection in ocular tissues by PCR.

In summary, the HHV family-DNA was detected by multiplex PCR in the ocular fluids of patients with various types of uveitis. Among the positive samples that were identified through the use of qualitative PCR, many of these samples showed significantly high copy numbers of HHV-DNA, when examined by real-time PCR. However, it should be noted that

Downloaded from bjo.bmj.com on 28 July 2008

levels of the viral load for some of the intraocular samples could not be detected, for example, as was seen for the real-time PCR measurement of EBV. Thus, a qualitative multiplex PCR might be a useful method for screening viral infections, and furthermore, quantitative real-time PCR might make it possible to evaluate the clinical relevance of virus infections.

Acknowledgements: We would like to thank S Horie and Y Futagami, for their technical assistance. This work was supported by a Grant-in-Aid for Young Scientists (B) 18791263 of the Ministry of Education, Culture, Sports, Science and Technology, Japan.

Competing interests: None.

Ethics approval: The research followed the tenets of the Declaration of Helsinki, and all study protocols were approved by the Institutional Ethics Committees of Tokyo Medical and Dental University.

Patient consent: Informed consent was obtained from each patient prior to sample collection.

REFERENCES

1. **Ohashi Y,** Yamamoto S, Nishida K, *et al*. Demonstration of herpes simplex virus DNA in idiopathic corneal endotheliopathy. *Am J Ophthalmol* 1991;**112**:419–23.
2. **Yamamoto S,** Tada R, Shimomura Y, *et al*. Detecting varicella-zoster virus DNA in iridocyclitis using polymerase chain reaction. *Arch Ophthalmol* 1995;**113**:1358–9.
3. **Nakamura N,** Tanabe M, Yamada Y, *et al*. Zoster sine herpete with bilateral ocular involvement. *Am J Ophthalmol* 2000;**129**:809–10.
4. **Koizumi N,** Yamasaki K, Kawasaki S, *et al*. Cytomegalovirus in aqueous humor from an eye with corneal endotheliitis. *Am J Ophthalmol* 2006;**141**:564–5.
5. **Arimura E,** Deai T, Maruyama K, *et al*. Herpes simplex virus-2 quantification by real-time polymerase chain reaction in acute retinal necrosis. *Jpn J Ophthalmol* 2005;**49**:64–5.
6. **Asano S,** Yoshikawa T, Kimura H, *et al*. Monitoring herpesvirus DNA in three cases of acute retinal necrosis by real-time PCR. *J Clin Virol* 2004;**29**:206–9.
7. **Chichili GR,** Athmanathan S, Farhatullah S, *et al*. Multiplex polymerase chain reaction for the detection of herpes simplex virus, varicella-zoster virus and cytomegalovirus in ocular specimens. *Curr Eye Res* 2003;**27**:85–90.
8. **Sugita S,** Iwanaga Y, Kawaguchi T, *et al*. Detection of herpesviruses genome by multiplex PCR and real-time PCR in ocular fluids of patients with acute retinal necrosis [in Japanese]. *Nippon Ganka Gakkai Zasshi* 2008;**112**:30–8.
9. **Corey L,** Huang ML, Selke S, *et al*. Differentiation of herpes simplex virus types 1 and 2 in clinical samples by a real-time taqman PCR assay. *J Med Virol* 2005;**76**:350–5.
10. **Kimura H,** Morita M, Yabuta Y, *et al*. Quantitative analysis of Epstein–Barr virus load by using a real-time PCR assay. *J Clin Microbiol* 1999;**37**:132–6.
11. **Gautheret-Dejean A,** Manichanh C, Thien-Ah-Koon F, *et al*. Development of a real-time polymerase chain reaction assay for the diagnosis of human herpesvirus-6 infection and application to bone marrow transplant patients. *J Virol Meth* 2002;**100**:27–35.
12. **Hara S,** Kimura H, Hoshino Y, *et al*. Detection of herpesvirus DNA in the serum of immunocompetent children. *Microbiol Immnol* 2002;**46**:177–80.
13. **Polstra AM,** van den Burg R, Goudsmit J, *et al*. Human herpesvirus 8 load in matched serum and plasma samples of patients with AIDS-associated Kaposi's sarcoma. *J Clin Microbiol* 2003;**41**:5488–91.
14. **Kido S,** Sugita S, Horie S, *et al*. Association of varicella-zoster virus (VZV) load in the aqueous humor with clinical manifestations of anterior uveitis in herpes zoster ophthalmicus and zoster sine herpete. *Br J Ophthalmol* 2008;**92**:505–8.
15. **Takahashi H,** Sugita S, Shimizu N, *et al*. A high viral load of Epstein–Barr virus (EBV) DNA in ocular fluids in a HLA-B27 negative acute anterior uveitis patient with psoriasis. *Jpn J Ophthalmol*. In press.
16. **Kawaguchi T,** Sugita S, Shimizu N, *et al*. Kinetics of aqueous flare, intraocular pressure and virus-DNA copies in a patient with cytomegalovirus iridocyclitis without retinitis. *Inter Ophthalmol* 2007;**27**:383–6.
17. **Sugita S,** Shimizu N, Kawaguchi T, *et al*. Identification of human herpesvirus 6 in a patient with severe unilateral panuveitis. *Arch Ophthalmol* 2007;**125**:1426–7.
18. **Elnifro EM,** Cooper RJ, Klapper PE, *et al*. Multiplex polymerase chain reaction for diagnosis of viral and chlamydial keratoconjunctivitis. *Invest Ophthalmol Vis Sci* 2000;**41**:1818–22.
19. **Druce J,** Catton M, Chibo D, *et al*. Utility of a multiplex PCR assay for detecting herpesvirus DNA in clinical samples. *J Clin Microbiol* 2002;**40**:1728–32.

From www.bloodjournal.org at TOKYO-IKA-SHIKA-DAIGAKU on December 10, 2009. For personal use only.

Aberrant overexpression of microRNAs activate AKT signaling via down-regulation of tumor suppressors in natural killer–cell lymphoma/leukemia

*Yasuo Yamanaka,[1] *Hiroyuki Tagawa,[1] Naoto Takahashi,[1] Atsushi Watanabe,[1] Yong-Mei Guo,[1] Keiko Iwamoto,[1] Junsuke Yamashita,[2] Hirobumi Saitoh,[1] Yoshihiro Kameoka,[1] Norio Shimizu,[3] Ryo Ichinohasama,[4] and Ken-ichi Sawada[1]

[1]Department of Hematology, Nephrology, and Rheumatology, Akita University Graduate School of Medicine, Akita; [2]Radioisotope Research Laboratory, Bioscience Education-Research Center, Akita University School of Medicine, Akita; [3]Division of Virology and Immunology, Medical Research Institute, Tokyo Medical and Dental University, Tokyo; and [4]Division of Histology, Tohoku University Graduate School of Medicine, Sendai, Japan

The gene(s) responsible for natural killer (NK)–cell lymphoma/leukemia have not been identified. In the present study, we found that in NK-cell lymphoma lines (n = 10) and specimens of primary lymphoma (n = 10), levels of miR-21 and miR-155 expression were inversely related and were significantly greater than those found in normal natural killer ($CD3^-CD56^+$) cells (n = 8). To determine the functions of these microRNAs in lymphomagenesis, we examined the effects of antisense oligonucleotides (ASOs) targeting miR-21 (ASO-21) and/or miR-155 (ASO-155) in NK-cell lymphoma lines overexpressing one or both of these miRNAs. Conversely, cells showing little endogenous expression of miR-21 or miR-155 were transduced by the use of lentiviral vectors, leading to their overexpression. Reducing expression of miR-21 or miR-155 led to up-regulation of phosphatase and tensin homologue (PTEN), programmed cell death 4 (PDCD4), or Src homology-2 domain-containing inositol 5-phosphatase 1 (SHIP1). ASO-21– and ASO-155–treated cell lines all showed down-regulation of phosphorylated AKT^{ser473}. Moreover, transduction with either miR-21 or miR-155 led to down-regulation of PTEN and PDCD4 or SHIP1 with up-regulation of phosphorylated AKT^{ser473}. Collectively, these results provide important new insight into the pathogenesis of NK-cell lymphoma/leukemia and suggest targeting miR-21 and/or miR-155 may represent a useful approach to treating NK-cell lymphoma/leukemia. (Blood. 2009;114: 3265-3275)

Introduction

Natural killer (NK)–cell lymphomas/leukemias are characterized groups of highly aggressive lymphoid malignancies, which are composed of "extranodal NK/T-cell lymphoma, nasal type" and "aggressive NK-cell leukemia."[1] Notably, these 2 subtypes show many similarities in their morphologic features, immunophenotypes, and genotypes and are invariably associated with Epstein-Barr virus (EBV), which suggests they may share the same genetic alterations. To assign a classification, the World Health Organization classification uses cytogenetic and molecular features to characterize lymphoma subtypes.[1] For example, it is known that various genomic translocations and genetic alterations, including BCL2, CCDN1, and c-MYC, occur in B-cell lymphomas. These disease-specific genetic translocations characterize lymphoma subtypes, such as follicular lymphoma characterized by BCL2 rearrangement, mantle-cell lymphoma characterized by CCDN1 rearrangement, and Burkitt lymphoma characterized by c-MYC rearrangement. However, although the World Health Organization classification recognizes NK-cell lymphomas/leukemias as distinct clinicopathologic entities, disease-specific translocations and the gene(s) affected in the 2 subtypes have not yet been identified. It was previously reported that a 6q deletion occurs in approximately 10% to 20% of NK-cell lymphomas/leukemias[2-7]; however, this loss may not be disease specific because it has been observed in a variety of cancers, including solid tumors and hematologic malignancies. It is currently unclear whether the loss is a primary or progression-associated event.

It was recently discovered that some microRNAs (miRNAs) are oncogenic in B-cell lymphomas. For example, aberrant overexpression of 2 miRNAs, miR-17-92 and miR-155, is closely associated with B-cell lymphomagenesis.[8] With respect to miR-17-92, we recently demonstrated that the polycistron can down-regulate CDKN1A/p21 in B-cell lymphomagenesis and promote cell-cycle regulation.[8] Furthermore, it is unlikely that aberrant expression of miRNAs is restricted to B-cell lymphomas, and it may occur in other lymphoma subtypes, including T/NK-cell lymphomas. In the present study, therefore, we used Northern and quantitative polymerase chain reaction (PCR) analyses to screen for and quantitatively assess miRNA expression in NK-cell lymphomas/leukemias and found that miR-21 and miR-155 were overexpressed in NK-cell lymphoma/leukemia. Moreover, the effects of antisense oligonucleotides (ASOs) revealed that miR-21 and miR-155 act as oncomiRNAs, promoting NK-cell lymphomagenesis through dysregulation of AKT signaling.

Methods

Cell lines

The following 10 NK-cell lymphoma/leukemia cell lines commonly show $CD2^+$, $sCD3^-$, $CD3\varepsilon^+$, $CD5^-$, $CD19^-$, $CD56^+$, $TCR\alpha/\beta^-$, and $TCR\gamma/\delta^-$ phenotypes: NKL, KHYG1, YT, NK92, HANK1, KAI3, SNK1, SNK6,

Submitted June 1, 2009; accepted July 22, 2009. Prepublished online as *Blood* First Edition paper, July 29, 2009; DOI 10.1182/blood-2009-06-222794.

*Y.Y. and H.T. share first authorship.

The online version of this article contains a data supplement.

The publication costs of this article were defrayed in part by page charge payment. Therefore, and solely to indicate this fact, this article is hereby marked "advertisement" in accordance with 18 USC section 1734.

© 2009 by The American Society of Hematology

From www.bloodjournal.org at TOKYO-IKA-SHIKA-DAIGAKU on December 10, 2009. For personal use only.

Table 1. Summary of primary NK-cell lymphoma/leukemia cases

Patient no.	Sex	Age	Diagnosis	Origin	EBER-ISH	sCD3	CD2	CD5	CD20	CD56	TCRre	Cytotoxic molecules
NKpt1	M	84	Extranodal NK/T-cell lymphoma, nasal type	Orbit	+	−	+	−	−	+	ND	TIA-1+, granzyme B+
NKpt2	M	57	Extranodal NK/T-cell lymphoma, nasal type	Skin	−	+	+	−	−	+	−	TIA-1+, granzyme B+
NKpt3	M	58	Aggressive NK-cell leukemia	Peripheral blood	+	−	+	−	−	+	ND	TIA-1−, granzyme B−
NKpt4	M	68	Extranodal NK/T-cell lymphoma, nasal type	Nasal cavity	+	+	+	−	−	+	ND	TIA-1+, granzyme B+
NKpt5	M	44	Extranodal NK/T-cell lymphoma, nasal type	Nasal cavity	+	−	+	−	−	+	−	TIA-1+, granzyme B+
NKpt6	M	53	Extranodal NK/T-cell lymphoma, nasal type	Nasal cavity	+	−	+	−	−	+	−	TIA-1+, granzyme B−
NKpt7	F	68	Extranodal NK/T-cell lymphoma, nasal type	Nasal cavity	ND	−	+	−	−	+	ND	TIA-1+, granzyme B+
NKpt8	M	60	Aggressive NK-cell leukemia	Bone marrow	+	−	+	−	−	+	−	ND
NKpt9	M	75	Extranodal NK/T-cell lymphoma, nasal type	Nasal cavity	+	−	+	−	−	+	ND	TIA-1+, granzyme B−
NKpt10	M	56	Aggressive NK-cell leukemia	Bone marrow	+	−	+	−	−	+	ND	TIA-1+, granzyme B+

EBER-ISH indicates EBER in situ hybridization; ND, not determined; NK, natural killer; TCRre, T-cell receptor rearrangement; +, positive stain; and −, negative stain.

DERL7, and MOTN1.[9-18] The culture medium was RPMI1640 supplemented with 10% fetal calf serum or 5% human serum with 200 U (NKL, KHYG1, YT, KAI3, NK92, HANK1, DERL7, and MOTN1) or 700 U (SNK1 and SNK6) of IL-2. Rat-1 was derived from rat fibroblasts that were obtained from the RIKEN Bioresource Center and cultured in Dulbecco modified Eagle medium supplemented with 10% fetal calf serum.

Primary NK-cell lymphoma/leukemia samples and normal sCD3$^-$ and CD56$^+$ cells

Ten specimens of primary NK-cell lymphoma/leukemia, including 7 "extranodal NK/T cell lymphoma, nasal type" and 3 "aggressive NK-cell leukemia," were collected from 10 patients (9 men and 1 woman, ranging in age from 44 to 82 years; Table 1). Samples were obtained from 10 patients with an Institutional Review Board of Akita University–approved protocol. Informed consent was obtained from all patients according to the Declaration of Helsinki before collection of the specimens. In addition, none of the patients had a history of malignant lymphoma/leukemia. All the samples were obtained from tumors at the time of diagnosis before any treatment was administered. All samples showed CD2 and CD56 positivity. Eight cases were also positive for CD3ε but negative for sCD3. All cases showed either EBER-ISH positive or cytotoxic molecules (TIA-1 or Granzyme B) positive or both. Normal sCD3$^-$CD56$^+$ cells also were collected from 8 healthy donors (3 women and 5 men; 3 of these 8 also were used as control samples in Northern blot analyses) by the use of a magnetic cell-sorting system (Miltenyi Biotec) with CD3–fluorescein isothiocyanate (FITC), CD19-FITC, and CD56-FITC antibodies and anti-FITC MicroBeads. Southern blot analysis was performed for 4 of 10 cases by the use of TCR-Cβ-1 probe.

Northern blot analysis

Northern blotting for mature microRNAs was performed as described elsewhere.[8] In brief, total RNA was extracted from the cell lines by the use of the acid-phenol precipitation method, after which 2-μg normal control samples or 5-μg cell line samples were separated on 15% denaturing polyacrylamide gels. The blots for all 4 membranes hybridized by γ^{32}-dATP (1.85 MBq per 10 pmol probe; for 5S tRNA, 1 pmol)–antisense oligo for microRNAs were exposed at the same conditions: 8 hours at −80°C with BioMax films (Kodak).

Western blot analysis

Western analyses were performed as described elsewhere.[8] Antibodies against phosphatase and tensin homologue (PTEN; A2B1) and Src homology-2 domain-containing inositol 5-phosphatase 1 (SHIP1; P1C1) were purchased from Santa Cruz Biotechnology. Antibodies against programmed cell death protein 4 (PDCD4), phospho-NFκB (phospho-p65^{ser536}; 93H1), phosphor-AKT ^{ser473} (pAKT), total AKT, Apaf-1, RECK (D8C7), p21$^{WAF1/CIP1}$ (p21), and p27^{KIP1} (p27) were all purchased from Cell Signaling Technology (Cell Cycle Regulation Sampler Kit). Anti-Bim (AAP-330) was from Stressgen Bioreagents. Anti-Bcl2 (BCL-2-100) was from Sigma. Anti-p53 (DO-7) was from Dako Cytomation.

Real-time quantitative PCR for miRNAs (Taqman PCR)

A Recover All Total Nucleic Acid Isolation kit (Applied Biosystems) was used to extract total RNA from primary specimens embedded in paraffin. Quantitative stem-loop reverse transcription (RT) was then performed by the use of a Taqman microRNA RT kit (Applied Biosystems), after which quantitative PCR for mature miRNAs was performed by the use of Taqman microRNA assays (Applied Biosystems). All reactions were run in duplicate. Mean cycle threshold (C_t) values for all miRNAs were quantified by the use of sequence detection system software (SDS, version 2.1; Applied Biosystems). The miRNA expression was normalized to U47 mRNA expression, yielding a $-\Delta C_t$ value. The $-\Delta\Delta C_t$ value was then calculated by subtracting the $-\Delta C_t$ value for a standard normal sCD3$^-$CD56$^+$ sample from the respective $-\Delta C_t$ values from the cancer cells. The $-\Delta\Delta C_t$ values were then imported into Microsoft Excel, and P values were calculated by the use of a Student t test. Quantitative RT-PCR was performed by the use of a Universal probe library (Roche Diagnostics) and Light Cycler 480 probe master (Roche Diagnostics) with the Taqman method.

Construction of plasmids and transduction

Lentiviral vectors for the delivery of microRNA were designed and produced by use of the reagents and protocols included in the BLOCK-iT Lentiviral Pol II miR RNA interference expression system (Invitrogen). The premicro-RNA (miR-21 and miR-155) and its reverse complement were annealed and ligated into the pcDNA6.2-GW/EmGFP-miR vector, which contains the full premicro-RNA 5′- and 3W′-flanking regions, as well as the cocistronic Emerald *GFP* (*EmGFP*) gene. After sequence verification, the EmGFP-premicro-RNA cassette was transferred to the pLenti6/V5 expression construct by the use of BP/LR recombination reactions. Three micrograms of the resulting pLenti6/EmGFP-premicro-RNA vector, together with 9 μg of ViraPower Packaging mix, was transfected by the use of Lipofectamine 2000 into 293FT producer cells. After overnight culture, medium was exchanged to remove transfection reagents. The following day, virus stocks were harvested. Viral supernatants were harvested 48 to 72 hours after transfection. Cells stably expressing miR-21 or miR-155 were sorted for green fluorescent protein (GFP) expression by the use of a

From www.bloodjournal.org at TOKYO-IKA-SHIKA-DAIGAKU on December 10, 2009. For personal use only.

Dako Cytomation MoFlo, after which individual clones were isolated. In Rat-1 cells, the pre miR-155 was cloned into the appropriate cloning site of pMXs^{puro}, after which Rat-1 cells were stably transfected. Detailed transfection methods was described elsewhere.[8]

ASO assay

ASO and their respective scrambled control oligonucleotides were synthesized as hybrid deoxyribonucleotide molecules linked between the 2′-O and 4′-C-methylene bridge (locked nucleic acid) modification of G and C residues (Greiner). The ASOs used were as follows: AS-miR-21 (ASO-21), 5′-TCAACATCAGTCTGATAAGCTA-3′ and AS-miR-155 (ASO-155), 5′-TCCCCTATACACGATTAGCATTAA-3′. The SCOs used were SC-miR-21 (SCO-21), 5′-TAACGTCACTTCGACTGAACTGCT-3′ and SC-miR-155 (SCO-155), 5′-ATCTCATACTACACTTGAACACT-3′. To assess their effects, cells were plated to a density of 10^5 cells/well in 24-well dishes and then transfected with oligonucleotides (20 nmol/L) by the use of Lipofectamine 2000 (day 1). Two days later (day 3), the cells were harvested and resuspended in a fresh medium. Then cells were transfected again with oligonucleotides (20 nmol/L) by the use of Lipofectamine 2000 by day 5 and analyzed.

Cell-cycle analysis

For cell-cycle analysis, the cells were suspended in a mixture containing 0.2 mL of 0.9% NaCl and 3 mL of 70% EtOH, after which the nuclei were stained with propidium iodide (Sigma). The cellular DNA content was then measured with a FACSCalibur flow cytometer running the CELL Quest program (BD Biosciences).

Apoptosis analysis

For apoptosis analysis, an annexin V–PE apoptosis detection kit (BD Biosciences) was used to assess the incidence of apoptosis among GFP-positive cells. In addition, an annexin V–FITC apoptosis detection kit (Sigma) was used to assess the incidence of apoptosis among GFP-negative cells. Cells were exposed by 50 μmol/L etoposide for 2 hours (KAI3 cells) or 100 μmol/L etoposide for 4 hours (NKL, YT, and MOTN1 cells), after which the assays were performed.

Luciferase reporter assay

The pGL3 control vector (Promega) encoding firefly luciferase was modified such that the *INPP5D/SHIP1* 3′UTR was inserted into the *Xba*I site immediately downstream from the stop codon. Rat-1 cells expressing miR-155 were cultured to 80% to 90% confluence in 24-well plates and then transfected with 0.8 μg of the firefly luciferase reporter vector and 0.16 μg of pRL-TK control vector (Promega) encoding Renilla luciferase with Lipofectamine 2000 in a final volume of 1.0 mL. Thirty hours later, firefly and Renilla luciferase activities were measured consecutively in Dual-luciferase assays (Promega). Two independent experiments were conducted in triplicate. In addition, the following sequences were inserted into the PGL3 control vector: wild-type *INPP5D/SHIP1* 3′UTR, 5′-CACCAGTTTAAAACGGTGTGTGTTCGGAGGGGTGAAAGCATTAA-GAAGCCCAGTGCCCTCCTGGAGTGAG-3′ (the underlined sequence is the conserved target of miR-155) and mutated INPP5D/SHIP1 3′ UTR, 5′-CACCAGTTTAAAACGGTGTGTGTTCGGAGGGGTGAAtGCATTAtGA-AGCCCAGTGCCCTCCTGGAGTGAG-3′ (mutations are indicated by lowercase characters).

Results

Detection of aberrant overexpression of microRNAs in NK-cell lymphoma/leukemia lines

To detect aberrant overexpression of miRNAs in NK-cell lymphomas/leukemias, we initially performed a Northern analysis with 66 probe sets (supplemental Table 1, available on the *Blood* website; see the Supplemental Materials link at the top of the online article) with 12 lymphoma/leukemia cell lines, which included 6 NK-cell, 2 T-cell, and 4 B-cell lymphomas/leukemias. The probe sets for the miRNAs were selected based on recent reports on cancer-associated miRNAs. We found that miR-21, miR-23a, miR-29 family (miR-29a-c), and miR-155 were all more highly expressed in NK-cell lymphoma cell lines than in B-cell lymphoma cell lines. miR-20, miR-26a, miR-92, miR-103, and miR-181 were also ubiquitously overexpressed in the examined samples.

Because our interest was to investigate NK-cell lymphoma–specific overexpression of miRNA, we further examined expression of miR-21, miR-23a, miR29 family (miR-29a-c), and miR-155 in 10 NK-cell lymphoma cell lines. We defined "overexpression" as a level of miRNA expression that was more than 2-fold greater than the average in corresponding normal cells. The expression levels of these 4 miRNAs in 2 T-cell lines, 6 B-cell lymphoma/leukemia lines, and 3 normal sCD3$^-$CD56$^+$ samples (control) are compared in Figure 1A-B. Expression of miR-21 and miR-155 in KAI3 cells was 4.7- to 8.8-fold greater than the average expression level observed in normal control cells (averages: 0.17 for miR-21; 0.36 for miR-155; Figure 1B). Expression of miR-21 in KAI3, YT, NK92, NKL, KHYG1, HANK1, SNK1, SNK6, and DERL7 was 3.1- to 15.7-fold greater than in normal control cells. miR-155 expression in KAI3, KHYG1, HANK1, SNK1, SNK6, and MOTN1 was 2.6- to 10.2-fold greater than in normal control cells (Figure 1A-B). Expression of miR-21 and miR-155 in these cell lines were overexpressed than normal control cells. By contrast, levels of miR-21 in MOTN1 cells and levels of miR-155 in YT, NK92, NKL, and DERL7 cell were the same or less than 2-fold lower than in control cells. Expression of miR-23a in KAI3 cells was similar to that in the normal control samples, whereas levels of miR-29a were slightly greater in the KAI3 cells than in the control samples.

Comparison of the miRNA expression in NK-cell lymphoma/leukemia lines revealed a significant inverse relation between the expression of miR-21 and miR-155 ($P = .017$; Figure 1C), but no significant relations were detected for any other miRNA pairs (eg, miR-21 vs miR-23a; data not shown). We next performed quantitative real-time PCR (Taqman PCR) by the use of 28 lymphoma cell lines, including 10 NK-cell, 4 T-cell, and 14 B-cell lymphoma/leukemia lines, as well as 8 normal control samples. These cell lines and control cells include all samples presented in Figure 1. Taqman PCR showed significantly greater expression of these miRNAs in the NK-cell and T-cell lymphoma/leukemia lines than in the B-cell lymphoma lines (Figure 2A), but there was no significant difference in their expression between NK-cell and T-cell lymphomas/leukemias. Moreover, Taqman PCR also showed an inverse correlation between the expression of miR-21 and miR-155 in the NK-cell lymphoma/leukemia cell lines (Figure 2B).

Overexpression of microRNAs in primary NK-cell lymphoma/leukemia cases

To examine the expression of candidate microRNAs in primary extranodal NK-cell lymphoma (Table 1), we extracted total RNA from paraffin-embedded tissues, from CD56$^+$ tumor cells (Figure 3A) collected by microscopic dissection. Aggressive NK-cell leukemia samples were obtained from peripheral blood or bone marrow. Total RNA from normal sCD3$^-$CD56$^+$ cells were obtained from peripheral blood samples collected from 8 healthy donors. Comparison of patient samples to normal sCD3$^-$CD56$^+$ cells revealed no significant differences in the expression of miR-23a and miR-29a (Figure 3B). We therefore excluded these

From www.bloodjournal.org at TOKYO-IKA-SHIKA-DAIGAKU on December 10, 2009. For personal use only.

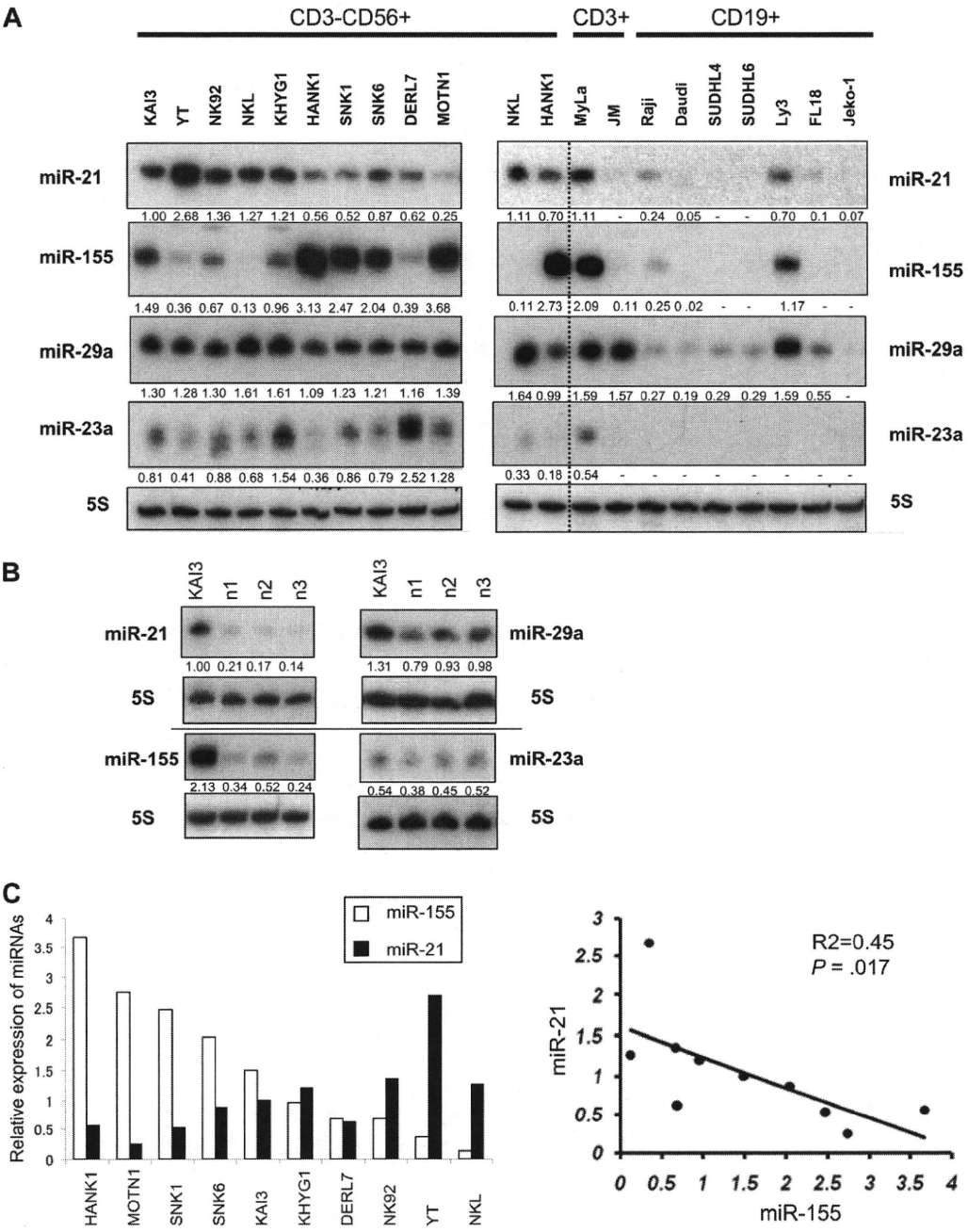

Figure 1. Northern analysis of miR-21, miR-23a, miR-29a, and miR-155 in NK-cell lymphoma/leukemia lines. (A) Northern analysis of miR-21, miR-23a, miR-29a, and miR-155 in 10 NK-cell ($CD3^-CD19^-CD56^+$; left panel), 2 T-cell ($CD3^+CD19^-CD56^-$; right panel), and 7 B-cell ($CD3^-CD19^+CD56^-$; right panel) lymphoma/leukemia lines. NKL and HANK1 are shown in both panels in duplicate to compare miRNA expressions. Fold changes in miRNA were determined by densitometry and are shown below the gels after normalization to the level of miR-21 in KAI3 cells, which was assigned a value of 1.00. The blots for all 4 membranes hybridized by γ^{32}-dATP-antisense oligo for microRNAs were exposed at the same condition (see "Methods"). (B) Expression of miR-21, miR-23a, miR-29a, and miR-155 measured in 3 samples of normal cells (n1, n2, and n3) expressing $sCD3^-CD56^+$. The level of miR-21 expression in KAI3 cells was assigned a value of 1.00. (C) Correlation between miR-21 and miR-155 expression. In the left panel, □ and ■ depict relative expression values for miR-155 and miR-21 expression, respectively. In the right panel, y-axis, expression values for miR-21 expression; x-axis, expression values for miR-155 expression. The *P* value was calculated by simple regression analysis.

miRNAs from further investigation. By contrast, miR-21 and miR-155 were expressed at significantly ($P < .001$) greater levels in cancer cells than normal $sCD3^-CD56^+$ cells (Figure 3B), and expression levels of miR-21 and miR-155 were also inversely related in primary specimens, as was observed in cell lines ($P = .001$; Figure 3C).

Our results demonstrated that miR-21, miR-155, or both were overexpressed in NK-cell lymphoma/leukemia lines and primary samples, although the overexpression of these miRNAs was not NK-cell lymphoma/leukemia specific (Figures 1-2).

miR-21 induces dysregulation of PTEN/AKT signaling in NK-cell lymphoma/leukemia

miR-21 and miR-155 are known to be oncogenic in a variety of cancers, including hematologic malignancies. To determine whether